Nickel Ferrite/Polyaniline Nanocomposite Doped with 2-Naphthalene Sulfonic Acid as Aqueous Chromium Adsorbent

By

Ruth Nzisi Kasavo

Dissertation submitted in partial fulfilment of the requirements for the degree of

Master of Engineering (Chemical Engineering)

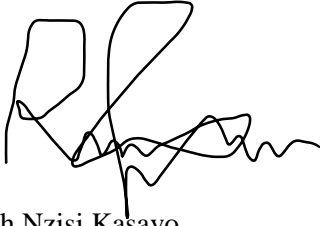In the faculty of Engineering, Built Environment and Information Technology

University of Pretoria

Pretoria

2023

Declaration

I Ruth Nzisi Kasavo, student number 15288057, do hereby declare that the dissertation, which I hereby submit for the degree Master of Engineering in Chemical Engineering at the University of Pretoria, is my own work and has not previously been submitted by me for a degree at this or any other tertiary institution.

Ruth Nzisi Kasavo

02 October 2023

Nickel Ferrite/Polyaniline Nanocomposite Doped with 2-Naphthalene Sulfonic Acid as Aqueous Chromium Adsorbent.

Student: Ruth Nzisi Kasavo

Supervisor: Prof. Hendrik G. Brink

Co-supervisor: Dr Madhumita Bhaumik

Department: Chemical Engineering

University: University of Pretoria

Degree: Master of Engineering (Chemical Engineering)

Abstract

Chromium is one of the most toxic heavy metals found in many industrial effluents due to its ability to easily enter the human body and cause serious health problems. In this study, the ability of a nanocomposite of nickel ferrite and polyaniline doped with 2-naphthalene sulfonic acid (PANINSA/NiFe$_2$O$_4$) to remove chromium (Cr (VI)) from synthetic wastewater was studied. The doping of the material with 2-NSA leads to the formation of tubular-shaped rods which increases the surface area of the material. Adsorption parameters such as solution pH, dosage of adsorbent, time of agitation, and initial concentration of pollutant were studied and optimized. The adsorption was highly dependent on solution pH with a maximum adsorption observed at pH 2. The results revealed a maximum removal of 99.9% from 50 mg/L Cr (VI) solution for a catalyst loading of 1 g/L. Freundlich, Langmuir and Two-Surface Langmuir non-linear isotherm models were fitted to the data. Kinetics studies revealed a fast adsorption process in the first 30 minutes followed by slower adsorption with maximum Cr (VI) removal achieved within 24 hours. The Two-Surface Langmuir model best described the isotherm data from the experiment. The effect of the temperature study revealed that the adsorption capacity for the Cr (VI) increased with an increase in temperature with the maximum adsorption capacity (420 mg/g) observed at 45 °C. The calculated thermodynamic parameters revealed endothermic and spontaneous adsorption process. The Cr (VI) removal mechanism was by electrostatic attraction, reduction, and surface complexation. The reusability studies showed that PANI-NSA/NiFe_2O$_4$ could be used for 5 cycles with a 99 % Cr (VI)removal from 50 mL solution containing 50 mg/L Cr (VI)in the first 2 cycles This study demonstrated that PANI-NSA/NiFe$_2$O$_4$ has a potential in the industrial application for removal of Cr (VI).

KEYWORDS: Polyaniline, nickel ferrite, chromium, adsorption, nanocomposite

Acknowledgements

First and foremost, I want to extend my deepest thanks to God for granting me the strength, perseverance, and wisdom to navigate through the challenges of this academic journey.

To my esteemed supervisor, Prof Deon Brink, your invaluable mentorship, continuous support, and insightful guidance throughout this research have been instrumental in shaping the trajectory of my dissertation. Your dedication to my academic growth has been truly remarkable.

I would also like to acknowledge my co-supervisor, Dr. Madhumita Bhaumik, for her unwavering commitment to my academic development. Your guidance, training, and invaluable assistance in data collection have been pivotal in enhancing the quality and depth of my research.

My heartfelt appreciation goes out to Ms. Alette Devega for her indispensable support with lab technicalities. Your expertise and assistance were invaluable in ensuring the smooth progression of my experiments.

I owe a debt of gratitude to my friend, Dr. Brian Gidudu, for his invaluable research input and insightful discussions. Your constructive feedback and collaborative spirit have greatly enriched my work.

I extend my deepest thanks to my family for their unwavering prayers, encouragement, and unconditional support throughout this academic endeavour. Your belief in me has been a constant source of motivation, and I am profoundly grateful for your love and encouragement.

Last but not least, I want to express my gratitude to the MasterCard Foundation Scholarship Program and National Research Fund (South Africa) for their generous financial support, which made this research possible. Your investment in my education has not only facilitated my academic growth but also contributed to the advancement of knowledge in my field.

To all those mentioned above, and to everyone who has played a part, no matter how small, in my journey towards completing this dissertation, I am deeply thankful. Your support and contributions have been invaluable, and I could not have reached this milestone without you.

Dedication

This work is dedicated to my mother, sisters, and any woman in my community who has been denied the opportunity to be great due to patriarchy.

Table of Contents

List of Figures

List of Tables

Chapter 1   Introduction

1.1 Background

Chromium (atomic number 24) is a steel-grey, lustrous, hard crystalline metal. It was first discovered by French chemist Louis Vauquelin in 1797. It is the 24th element in the Periodic Table with the symbol Cr and is situated between vanadium and manganese and belongs to transition group VI-B of with a ground-state electronic configuration of $Ar33d^54s^1$ along with molybdenum and tungsten (Giri, 2012). Chromium comprises about 0.037 percent of the earth's crust and it is twenty-first most naturally abundant element on earth's crust with the highest reserves found in South Africa and Kazakhstan (Coetzee *et al*, 2020).

In aqueous solutions and natural environment, chromium is mostly found in two oxidation states: trivalent (Cr (III)) and hexavalent (Cr (VI)). Cr (III) occurs naturally in the environment and is not considered a health hazard because it forms a precipitate with soil colloids thus making it stable. On the contrary, $Cr(VI)$ which includes chromate (CrO_4^{2-}) and dichromate compounds ($Cr_2O_7^{2-}$) is an oxidizing agent which is has high solubility thus a high presence in wastewater and soils (Xia *et al*, 2019). While Cr (III)in water is mainly from natural sources such as soil erosion, volcanic activity and weathering of rocks and minerals, occurrence of Cr (VI)in water is mainly driven by anthropogenic release from chemical and manufacturing industries such as nuclear plants, leather tanning, metal plating, electroplating and current production, paints pigments, paper and dyes production (Affairs, 2012; Liu and Yu, 2020; Rakhunde *et al*, 2012). Incompletely processed chromite ores is another major source of environmental pollution by Cr (VI) (Zhitkovich, 2011).

Occupational exposure to Cr (VI) has been found to increase the risk of respiratory system cancer with both soluble and poorly soluble chromates being carcinogenic (Agarwal and Singh, 2017; Sharma *et al*, 2021; Zhitkovich, 2011). In addition to that, Cr (VI) disguises itself as oxyanions such as sulphate, carboxylate and phosphate which are needed by the body and diffuses through cell membranes causing damage to cellular proteins, lipid, and other organelles (Jahan *et al*, 2018), (Shekhawat *et al*, 2015). Due to the toxicity of Cr (VI), United states Environmental Protection Agency (USEPA) has imposed Cr (VI) discharge into inland water to a maximum concentration of 0.1 mg/L and a maximum concentration of 0.05 mg/L in portable water (Demirbas *et al*, 2004). In South Africa, Cr (VI) limit in drinking water is 0.05 mg/L while total chromium limit is 2 mg/L (Coetzee *et al*, 2020). It is therefore important to treat industrial waste before discharging it to the environment to ensure Cr (VI) concentration does not exceed the maximum allowable limits prescribed by water quality standards.

Several treatment methods have been used in the removal of Cr (VI) from industrial wastewater. These include photocatalysis (Arslan *et al*, 2022), phytoremediation (Panneerselvam and Priya K, 2023), biological/microbial remediation (Gautam *et al*, 2021) and electro-chemical reduction (Pi *et al*, 2021), and electro-coagulation (Lu *et al*, 2022). These methods often have limitations such as large volume of sludge which makes the process cost and energy intensive. Additionally, these methods suffer from low

1

removal efficiency. Adsorption treatment technology shows advantages over traditional methods due to its simplicity, high efficiency in removing heavy metals, and low cost (Geng *et al*, 2022; Khurshid *et al*, 2022). Additionally, when an adsorption method is used, the material can be recovered and recycled through desorption (Kera *et al*, 2017). Different adsorbents have been used for the removal of Cr (VI) from wastewater. These include chitosan based adsorbents (Liu *et al*, 2023b), carbon materials such as activated carbon (Abushawish *et al*, 2022), carbon nano-tubes (Feng *et al*, 2022), metal-organic frameworks (Yuan *et al*, 2022), modified rice husk (Lala *et al*, 2023), and $FeCl_3$-modified biochar (Hu *et al*, 2024).

Natural polymers such as polyaniline (PANI) and polypyrrole have been widely used as adsorbents in the removal of heavy metals from wastewater. PANI has gained widespread interest due to its high conductivity, large surface area, ease of synthesis, stability in environment, low cost of synthesis etc (Agrawal and Singh, 2016; Singh *et al*, 2019). Additionally, polyaniline contains large amounts of amino and imine groups (functional group containing a carbon-nitrogen double bond) which have a strong affinity for Cr (VI) and ability to reduce Cr (VI) to Cr (III) (Hsini *et al*, 2021; Lei *et al*, 2020). However, due to their amorphous structure, many polymers have been difficult to recover and recycle, restricting their application in industrial wastewater treatment. To overcome these challenges, researchers have been using composites of polymers with other materials such as nanoparticles. Nanoparticles are preferred due to their small size which increases the surface area of the nanocomposite. (Chávez-Guajardo *et al*, 2015) used polyaniline/maghemite and polypyrrole/maghemite magnetic nanocomposites for the removal of Cr (VI) and Cu (II) from aqueous media. (Rezvani *et al*, 2014) used a polyaniline-magnetite nanocomposite synthesized by the polymerization of aniline in the presence of magnetite nanoparticles as an ion exchange sorbent for the removal of Cr (VI) ions. In a recent study conducted by Lohrentz and others (Lohrentz *et al*, 2023) a nanocomposite of polyaniline and zero-valent nickel was used for hexavalent chromium removal.

There are limited studies on the application of polyaniline and nickel ferrite nanocomposites in the removal of chromium from aqueous solutions. Even though Agrawal and Singh (2016) used $NiFe_2O_4$-PANI nanocomposite in a previous study, they reported a very low maximum adsorption capacity (12.19 mg/g). The current study seeks to study the feasibility of using an improved nanocomposite of polyaniline and nickel ferrite in the removal of Cr (VI) from wastewater.

1.2 Problem statement

One of the most hazardous metals is used in many industries due to its desirable properties. Chromium is known for its wide applications in chrome plating, mining, leather industries, chemical industries among others (Liu and Yu, 2021; Pushkar *et al*, 2021). In addition to anthropogenic sources, chromium is released to the environment by natural activities such as volcanic eruption, soil erosion and rock weathering. The most common form of chromium, hexavalent chromium, is toxic and hazardous to living things. Due to its high solubility, this form of chromium easily finds its way to animal's tissue through feeding on contaminated animal feeds (Shekhar Sarker *et al*, 2023).

Traditional methods such as chemical precipitation (Minas *et al*, 2017), ion exchange (Han *et al*, 2020), membrane filtration (Semghouni *et al*, 2020), electro-chemical reduction (Pi *et al*, 2021), and oxidation-coagulation (Bora and Dutta, 2019) have been used in the removal of Cr(VI) from water. However, the methods have limitations such as large volume of sludge which makes the process costly and energy intensive and suffers from low efficiencies. Adsorption technology has advantages over the traditional methods due to its high efficiency in removing heavy metals, low cost, and ease of operation (Bhaumik *et al*, 2013; Jiang *et al*, 2018). Due to the limitations associated with adsorption materials, there is a pressing need to explore innovative and sustainable materials and technologies for the efficient removal of chromium from aqueous solutions.

Polyaniline nanocomposites doped with 2-naphthalene sulfonic acid have shown promise as potential adsorbents for aqueous chromium ions (Bhaumik *et al*, 2018; Lohrentz *et al*, 2023). However, several critical research gaps exist in this field that require in-depth investigation. Therefore, there is a need for further investigation on the use of doped polyaniline nanocomposites in the removal of Cr (VI) from wastewater.

1.3 Aims and objectives

In the current study, the effectiveness of 2-naphthalene sulfonic acid (2-NSA) doped polyaniline and nickel ferrite particle nanocomposite (PANI-NSA/NiFe$_2$O$_4$) produced via an *in situ* chemical oxidative polymerization method in removing of Cr(VI) from aqueous solution will be investigated. The following are the objectives of this study:

1. Determine physical and chemical properties of PANI-NSA/ NiFe$_2$O$_4$ and its constituents.
2. Determine optimum conditions for the process in terms of pH, adsorbent dosage, initial Cr(VI) concentration, contact time, and temperature.
3. Model the kinetics and thermodynamics of the Cr(VI) adsorption process.
4. Study the regeneration and recyclability of PANI-NSA/ NiFe$_2$O$_4$.

1.4 Structure of dissertation

Chapter 1 acts to introduce to the study. It will briefly discuss the pollution of water by Cr(VI), the different technologies applied in the removal of Cr(VI) from wastewater, the challenges with these technologies and why adsorption is the preferred method. The objectives of the study will also be defined in this chapter. Chapter 2 focuses on the literature review for this study and will include literature on the pollutant (Chromium), the method of removal (adsorption process) and the adsorbent (PANI-NSA/NiFe$_2$O$_4$). Chapter 3 discusses materials and methods, experimental procedures, characterization techniques and analysis procedures applied in this study. Chapter 4 presents results from this study, discusses the findings, and compares with other studies previously investigating chromium removal from wastewater. Chapter 5 provides the conclusions and recommendations based on the results from chapter 4. The reference bibliography will follow chapter 5. **The information in**

chapter 3 and 4 has been accepted for publishing in the Journal of Environmental Chemical Engineering.

Chapter 2   Literature review

2.1 Sources and effects of water pollution

Water is a natural resource covering most of the earth's surface. Nature has a way of purifying and recycling water sources and thereby providing enough clean water for human consumption. Water pollution is referred to as the presence of chemical, physical, or biological elements in a water body that may cause impairment with respect to beneficial usage (Schweitzer and Noblet, 2018). Due to an increase in human population growth and industrialization water pollution has become one of the main environmental problems that affects both humans and other species of the ecosystem around the world (Malik *et al*, 2022; Nasar and Mashkoor, 2019). Sources of water pollution are classified mainly into anthropogenic and natural sources. Anthropogenic sources are due to human activities such as agricultural activities, improper waste disposal and management, etc while natural sources are due to natural sources like volcanic activities.

2.1.1   Anthropogenic sources

2.1.1.1   Industrial waste

Industrial wastewater is the major source of water pollution due to the large volumes of effluents containing different pollutants being released from industries to rivers and water sources (Carolin *et al*, 2017). Industries such as textile, paper, apparel industries discharge harmful chemicals, and pollutants into water bodies (Farhan *et al*, 2023). According to the World Bank, the textile finishing and dyeing industries account for between 17 and 20 percent of the total water pollution (Rafiq *et al*, 2021). Dyes lead to the discoloration of water rendering it unconducive for human consumption and tourism-related activities. Heavy metals such as arsenic, mercury, and cadmium are also released from these industries, and they can lead to death even at very low concentration. Discharge of effluents into water bodies leads to the decrease in dissolved oxygen due to enhanced oxygen consumption arising from decomposition of dead organic matter. This leads to death and decrease of living organisms in the water bodies as a result of hypoxia (Haseena *et al*, 2017; Owa, 2013). In addition, discharge of hot water from industries leads to an increase in water temperature and consequently a decrease in organism activity in the water bodies by significantly affecting behavioural changes.

2.1.1.2   Agricultural activities

Pesticides, herbicides, and fertilizers used in agriculture can leach into groundwater and nearby water bodies, leading to contamination (Singh *et al*, 2022). Runoffs from agricultural farmlands enrich water bodies with nutrients which may lead to overgrowth of algae and other aquatic weeds (Ghangrekar and Chatterjee, 2018). Animal waste from livestock farms is another source of agricultural water pollution (Owa, 2013). Solids contained in these wastes block the penetration of sun hence limiting the growth of bottom plants in aquatic systems (Ghangrekar and Chatterjee, 2018).

2.1.1.3   Domestic and Municipal Wastewater

Sewage and wastewater from households can cause pollution if they are released into water sources without proper treatment. In addition, a large number of plastics are used for domestic purposes. Some of these plastics find their way to waste sources and environment causing more pollution. Some household products may also contain pollutants such as dyes, pharmaceuticals, acids, and even heavy metals. Due to the high cost of infrastructure required for the treatment of sewage and wastewater, many cities do not treat their domestic and municipal wastewater to meet the requirements before discharge (Mema, 2010; Onu *et al*, 2023).

2.1.2   Natural sources

Some heavy metals such as chromium are found in ores deposits which naturally exist on earth's surface. According to (Coetzee *et al*, 2020) chromium in rocks exists mainly as chromite which is formed by solidification of molten lava and the concentration can be as high as 400 ppm. These can find their way to water sources through soil erosion, weathering of rocks and volcanic activities hence causing water pollution by heavy metals. Although chromium exists mainly as Cr (III) in the environment, it can be oxidized to Cr (VI) in the presence of other minerals (Tumolo *et al*, 2020). The latter is toxic and more soluble hence easy to reach groundwater and cause more pollution (Oliveira, 2012). A summary of sources of water pollution is shown in Figure *2-1*.

2.2 Classification of water pollutants

Water pollutants can generally be classified into organic and inorganic pollutants. Organic pollutants include pesticides, insecticides, fertilizers, pharmaceuticals, industrial solvents, dyes, and wastes from food manufacturing. Inorganic pollutants include heavy metals, inorganic salts, trace elements and mineral acids released from industries (Rao *et al*, 2012; Schweitzer and Noblet, 2018). While organic pollutants can easily be broken down by microbes to form less harmful end-products (biodegrade), inorganic pollutants are non-biodegradable and thus their concentration in the environment will keep on increasing (Masindi and Muedi, 2018). In this research the focus will be on water pollution by heavy metals.

2.3 Heavy metals in wastewater

According to Bánfalvi (2011), a heavy metal is an element with a density five times heavier than that of water and a molar mass between 63.5 and 200.6. Even in parts per billion (ppb), heavy metals can still be harmful. Some examples of heavy metals are lead, mercury, arsenic, nickel, cadmium, chromium, cobalt, and zinc. Heavy metals in wastewater have become a significant environmental issue in recent years. Heavy metals cause substantial damage to ecosystems and human health at high concentrations. Due to their non-biodegradability, heavy metals accumulate in the ecosystem causing more environmental concerns (Carolin *et al*, 2017; Masindi and Muedi, 2018). The widespread application of heavy metals in numerous sectors and technological fields has increased the amount of heavy metals released into the environment. The burning of fossil fuels releases nickel, vanadium, mercury, selenium, and tin. Other important anthropogenic sources such as smelting and automobile

6

exhaust cause water pollution by heavy metals (Masindi and Muedi, 2018). Numerous natural processes such as weathering of rocks and soils and volcanic eruptions have also been major contributors of water pollution by both organic and inorganic pollutants. Processing and exploitation of metal pollutants has led to water pollution by heavy metals such as chromium, cadmium, copper, zinc, lead, mercury, and nickel (Farhan *et al*, 2023; Malik *et al*, 2022).

Even though industrial effluents should be treated to meet the requirements before discharge, some industries do not treat their wastes to meet the criteria due to the high cost of the process. This has led to discharge and accumulation of heavy metals in water and soil (Ranade and Bhandari, 2014). Once they accumulate in soil, heavy metals can slow down the decomposition of organic pollutants, hence increasing the soil pollution (Masindi and Muedi, 2018).
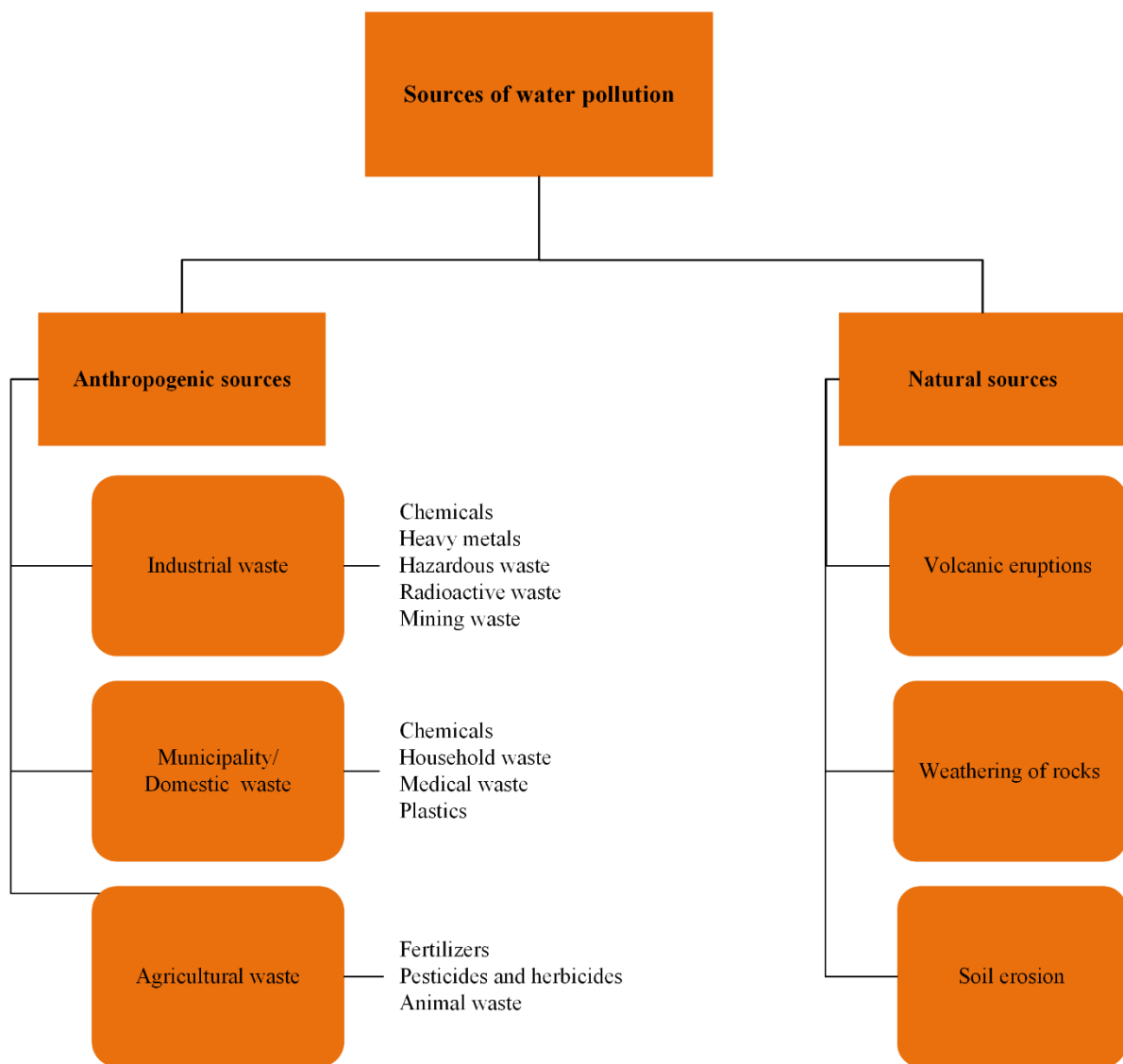
Figure 2-1: Sources of water pollution

Table 2-1: sources and effects of heavy metal pollution

Heavy metal	Sources	Health effects	Reference
Arsenic	Mining, smelting, burning fossil fuels, making glass and semiconductors, fertilizer production, weathering of rocks and volcanic eruption	Cardiovascular effects, cancer, diabetes, early life defects.	Khan *et al* (2020); Rahman and Singh (2019)
Cadmium	Plating, cadmium-nickel batteries, stabilizers, and alloys.	Lung cancer, cardiovascular effects	Carolin *et al* (2017); Pratush *et al* (2018)
Mercury	Paper and pulp, plastics, chloro-alkali, pharmaceutical, and oil refineries industries	Irritability, cognitive loss, lung damage, nausea, death	Carolin *et al* (2017); Zaynab *et al* (2022)
Lead	Electroplating, battery manufacturing, combustion of automobile fuel, paint, and pigment manufacturing	Fatigue, insomnia, hallucinations, headaches, stomach discomfort	Bhaumik *et al* (2021); Zaynab *et al* (2022)
Chromium	Leather industries, tanning industries, electroplating industries, textile industries	Acute toxicity, birth defects, decline in reproductive health, cancer.	Carolin *et al* (2017); Oruko *et al* (2020)

2.4 Chromium

"Chromium (atomic number 24) is a steel-grey, lustrous, hard crystalline metal " (Giri, 2012). It was first discovered by French chemist Louis Vauquelin in 1797. It is the 24th element in the Periodic Table with the symbol Cr. The metal belongs to transition group VI-B with a ground-state electronic configuration of $Ar33d^54s^1$ along with molybdenum and tungsten (Coetzee *et al*, 2020). Chromium comprises about 0.037 percent of the earth's crust. It is the twenty-first most naturally abundant element on earth's crust with the highest reserves being found in South Africa and Kazakhstan (Coetzee *et al*, 2020)

Chromium is mostly found in two oxidation states in aqueous and natural environment: trivalent (Cr (III)) and hexavalent (Cr (VI)). Cr (III) occurs naturally in the environment. It is not considered a health hazard because it forms a precipitate with soil colloids thus making it stable. On the contrary, Cr (VI) which includes chromate (CrO_4^{2-}) and dichromate compounds ($Cr_2O_7^{2-}$) is an oxidizing agent with high solubility which leads to its high presence in wastewater and soils (Xia *et al*, 2019).

2.4.1   Chromium in environment

While Cr (III) in water is mainly from natural sources such as soil erosion, volcanic activity and weathering of rocks and minerals, occurrence of Cr (VI) in water is mainly driven by anthropogenic release from chemical and manufacturing industries such as nuclear plants, leather tanning, metal plating, electroplating and current production, paints pigments, paper and dyes production (Liu and Yu, 2020), (Rakhunde *et al*, 2012). Incompletely processed chromite ores is another major source of environmental pollution by Cr (VI) (Zhitkovich, 2011). Occupational sources of chromium include anti-algae agents, antifreeze, chrome alloy production, cement production, chrome electroplating, porcelain and ceramics manufacturing, leather tanning, textile manufacturing and welding of alloys or steel (Giri, 2012).

Occupational exposure to Cr (VI) has been found to increase the probability of getting respiratory system cancer with both Cr (VI) and Cr (III) being carcinogenic (Agarwal and Singh, 2017; Sharma *et al*, 2021; Zhitkovich, 2011). In addition to that, Cr (VI) disguises itself as oxyanions such as sulphate, carboxylate and phosphate which are needed by the body and diffuses through cell membranes causing damage to cellular proteins, lipids, and other organelles (Chatterjee *et al*, 2014; Jahan *et al*, 2018). A maximum limit for Cr (VI) in discharge into inland water is 0.1 mg/L and 0.05 mg/L in portal water is allowed by the United states Environmental Protection Agency (USEPA) (Giri, 2012). It is therefore important to treat wastewater before discharging it to the environment to ensure Cr (VI) concentration does not exceed the prescribed maximum limits.

2.5 Traditional methods of removing heavy metals from wastewater

Heavy metal pollutants can be removed by biological, physical, and chemical methods.

Various traditional methods have been previously used to remove heavy metals from industrial wastewaters. Among these, chemical precipitation, ion exchange, membrane filtration, photocatalysis, chemical and electrical reduction and coagulation have widely been studied (Minas *et al*, 2017; Peng and Guo, 2020; Semghouni *et al*, 2020). These methods have often shown limitations such as large volume of sludge which makes the process cost intensive, high-energy costs and low efficiency (Agarwal and Singh, 2017; Arbabi *et al*, 2015; Peng *et al*, 2018). Due to this, these methods have not been able to effectively remove inorganic pollutants such as heavy metals. Table *2-2* discusses the advantages and disadvantages of traditional methods of water treatment.

2.5.1   Chemical Precipitation

According to Arbabi *et al* (2015), the most common method of removing heavy metals from contaminated water is chemical precipitation. It uses pH adjustment to change heavy metal ions into less soluble compounds like hydroxide, sulfide, carbonates, or other compounds (Fungene *et al*, 2023). These less soluble compounds can then be removed physically using techniques like sedimentation, flotation, or filtration (Azimi *et al*, 2017). The Chemical precipitation method has been demonstrated to be effective in remediation of heavy metals such as chromium, lead, copper, arsenic, and zinc. However, if the heavy metal ion concentration is too low, or if there are other metal ions present, the

9

method may not be effective depending on the chemical used. In addition, chemical precipitation requires addition of chemicals which leads to production of large volumes of sludge (Azimi *et al*, 2017; Dąbrowski *et al*, 2004).

2.5.2 Ion exchange

Ion exchange is a process where charged ions from a solution are taken up by solid materials and replaced with an equivalent number from another ionic species (Coetzee *et al*, 2020). Ion exchange involves removing different ions from the solution by using a solid matrix whose surface has extra but same charge as the ions being removed. The main benefit of employing this technology is that it can manage the relatively big volume while removing parts per billion (ppb) levels. In addition, this method can be used to remove both cations and anions (Shrestha *et al*, 2021). According to Razzak *et al* (2022) ion exchange has a number of benefits, such as the ability to handle high volumes of effluents simultaneously and the enhanced effectiveness in the remediation of heavy metals pollutants. Ion-exchange is an expensive method and it cannot handle very high concentrations of metal ions due to spoiling of the matrix that is used in the process (Arbabi *et al*, 2015). This limits its application for industrial wastewater treatment.

2.5.3 Membrane filtration

Membrane filtration is a technology that uses a membrane to separate substrates by application of pressure across the membrane. Examples of membrane filtration are reverse osmosis, microfiltration, nanofiltration, ultrafiltration, and electrodialysis (Keng *et al*, 2014). Reverse osmosis is a membrane technology which works by forcing solvent molecules through a semipermeable membrane against the concentration gradient thus separating the stream into a purified stream and a concentrated stream. This method is effective and cost effective in removing pollutants. However, reverse osmosis membranes are very susceptible to fouling due to deposition of the pollutants and concentration polarization on the membrane surface. This fouling leads to decline in the flux through the membranes

and thus, the quality of the water produced may be affected. In their study on the efficiency of reverse osmosis in the removal of four heavy metals (lead, chromium, cadmium and zinc) from hospital dialysis feed water, Pirsaheb and colleagues (Pirsaheb *et al*, 2014) found that reverse osmosis was able to decrease zinc concentration to moderate and chromium concentration to lower levels. However, the process was not effective in the removal of lead and cadmium. Periodic washing and replacing of membranes were therefore required.

2.5.4 Coagulation and flocculation

Coagulation is one of the most extensively used methods used for heavy metal removal due to its simplicity and effectiveness. The method involves the addition of a chemical (known as the coagulant) into the polluted solution. The coagulant neutralizes the charge on the pollutant causing them on to destabilize and form flocculants which are removed by flocculation (Razzak *et al*, 2022).

2.5.5 Electrochemical treatment

The most common electrochemical treatment method is electrodialysis. According to (Strathmann, 2010), electrodialysis has been used for more than 50 years to produce clean water from brackish water sources. Cation-selective and anion-selective membranes are alternately placed in the course of an electric current in the electrodialysis technique. Anions flow through the anion-exchange membrane layer in one direction while cations flow through the cation-exchanging membrane layer in the other way when current is applied. As a result, one side has a decrease in salinity while the other experiences a rise in salinity (Driscoll *et al*, 2008). Water is then passed through the membranes until all the salinity is removed. Electrodialysis is mostly used in combination with other methods such as ion-exchange when producing high-quality industrial process water or treating specific effluents (Strathmann, 2010).

2.5.6 Biological treatment

In biological degradation, a chemical removed from the environment by living things, typically microorganisms, such as bacteria and fungi that exist naturally in soil and water. Biological degradation is often accompanied by chemical oxidation. The chemical oxidation is applied as a pre-treatment method to reduce waste into biodegradable intermediates which are then treated through a biological process (Wang *et al*, 2013).

Table 2-2: Conventional methods used in the removal of heavy metals from wastewater

Method	Advantages	Disadvantages	Reference
Chemical precipitation	• Less energy requirements. • High efficiency. • Easy to operate.	• Chemicals added lead to large volumes of sludge which can lead to secondary pollution. • Cost intensive.	(Azimi *et al*, 2017; Dąbrowski *et al*, 2004)
Ion exchange	• Low cost. • High selectivity. • High efficiency. • Low volume of sludge.	• Cost intensive. • Sensitive to pH of the solution. • Cannot handle very high concentrations due to spoiling of the matrix.	(Arbabi *et al*, 2015; Razzak *et al*, 2022)
Membrane filtration	• Small operation space required. • Low solid waste. • Rapid operation. • No chemicals required.	• High energy consumption. • High cost of operation. • Not effective at low solute concentration.	(Mulvany, 1969; Pirsaheb *et al*, 2014)
Electrochemical treatment	• Versatile. • Does not require pH control. • Effective water treatment for small communities. • Cost-effective	• Requires addition of chemicals such as coagulants. • Treatment of sludge leads to increased cost of operation. • High investment cost. • High energy requirement.	(Radjenovic and Sedlak, 2015; Strathmann, 2010)
Biological treatment	• Economical. • High efficiency for organic matter removal. • Suspended solids can be removed. • Ease of operation.	• Results in large volume of biological sludge. • The process is slow. • Requires management and maintenance of microorganisms.	(Durai and Rajasimman, 2011; Sarayu and Sandhya, 2012)

11

2.6 Adsorption

In the recent years, research of new ways of treating wastewaters has gained mileage with researchers looking into application of technology in the water treatment. Adsorption is a traditional technology that outperforms the other traditional methods in terms of efficiency in the removal of heavy metals, cost, and convenience of use. Additionally, in many instances, when adsorption method is used, the material can be recovered and recycled through a desorption process (Bhaumik *et al*, 2013; Jiang *et al*, 2018; Kera *et al*, 2017). The first quantitative findings were made by Scheele (Scheele, 1777) and Fontana (Fontana, 1777) in 1773 and 1777, respectively, who reported several experiments on the uptake of gases by charcoal and clays. Later, de Saussure discovered that heat was generated during the process and that the solid material's porosity is what caused the adsorption process to occur (de Saussure, 1812).

Worch (2021) defines adsorption as a phase transfer process in which chemical species are removed from a fluid phase by attaching onto a solid surface. In water and wastewater treatment, adsorption involves removal of pollutants by attachment onto the surface of a solid material as either ions or molecules. The solid material on to which the chemical species being removed attaches is called adsorbent while adsorbate is the chemical species that is removed by adsorption (Rashed, 2013). In heavy metals adsorption, there are primarily three sequential steps: heavy metal transport from the bulk solution to the absorbent surface, followed by adsorption on particle surfaces, and finally, transportation within the adsorbent particle (Shrestha *et al*, 2021). Adsorption often coexists with desorption- a process in which the adsorbate is transferred from the adsorbent surface back to the solution. Figure *2-2* shows an illustration of terms used in adsorption.
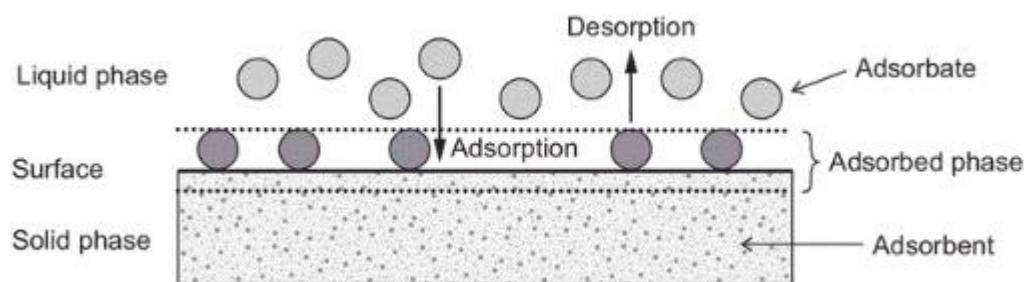
Figure 2-2: Adsorption terms (Worch, 2021).

There are two main categories of adsorption, physical adsorption and chemical adsorption (Hu and Xu, 2020). In physical adsorption, the increase in the adsorbate amount on the surface of the adsorbent is due to interaction of intermolecular forces namely van der Waals forces and its thermal effect is small. Because intermolecular attraction is weak, there is hardly any changes to the adsorbate molecules and physical adsorption is therefore reversible. On the other hand, in chemical adsorption also referred to

12

as chemisorption, the adsorbate reacts with the adsorbent leading to creation of covalent or ion bonds. The process is irreversible and with high amount of heat being released (Webb, 2003). Additionally, the activation energy required is larger in chemical adsorption. In order to describe the extent and quality of the adsorption process, equilibrium isotherms, kinetic models, and thermodynamic parameters such as Gibbs free energy are used (Gupta *et al*, 2021).

2.6.1   Adsorption isotherms

Adsorption is affected by the availability of pollutants and adsorbent. The interactions between adsorbent and the contaminant can be understood by studying the adsorption isotherms (Anjum *et al*, 2023). Adsorption isotherms are used to check the effect of changing the initial concentration of the contaminant on the removal of the contaminant at a constant temperature. Various adsorption isotherm models such as Langmuir, Freundlich, Dubinin-Radushkevitch and Temkin isotherm models have been applied by researchers in fitting of adsorption data (Muhammad *et al*, 2020). The most commonly studied isotherm models are Langmuir and Freundlich models.

2.6.1.1   Langmuir isotherm model

Langmuir isotherm model was originally developed for gas-solid-phase adsorption on activated carbon (Langmuir, 1918). With time, Langmuir isotherm model has been used to describe adsorption in liquid phases and on other adsorbents. The Langmuir isotherm is the most fitted isotherm model and assumes that a monolayer of the pollutant is adsorbed on to a homogeneous surface of the adsorbent with uniform distribution of energy. Additionally, the model assumes presence of fixed identical number of adsorption sites with equal affinity for the adsorbate (Hu *et al*, 2023). The non-linearized form of the Langmuir model is expressed in Equation (*2-1*):

$$Q_e = \frac{K_L Q_{max} C_e}{1 + K_L C_e} \tag{2-1}$$

Where Q_{max} is the maximum adsorption capacity (mg/g), k_L is the Langmuir adsorption equilibrium constant (L/mg) and C_e is the equilibrium concentration of the pollutant in the solution (mg/L). The maximum adsorption capacity and the adsorption equilibrium constant parameters are fitted from the isotherm model. The linear form of the Langmuir model is expressed by Equation

(2-2):

$$\frac{C_e}{Q_e} = \frac{1}{Q_{max}} C_e + \frac{1}{Q_{max} K_L} \tag{2-2}$$

When using the linear form of the model, a linear plot of C_e/Q_e against C_e should give a straight line with a high coefficient of regression (approaching 1) if the data is best described by the model (Olafadehan *et al*, 2022). To determine the suitability of the Langmuir isotherm and efficiency of the adsorption process, a dimensionless constant known as separation factor R_L is calculated from the Langmuir isotherm parameters (Ayawei *et al*, 2017):

$$R_L = \frac{1}{1 + K_L C_O} \tag{2-3}$$

Where C_O is the initial concentration of adsorbate (mg/L). When the value of $R_L > 1$, the adsorption process is unfavourable, $0 < R_L < 1$, favourable, $R_L = 1$ linear and $R_L = 0$ irreversible. Many researchers use the linear form of the Langmuir model due to its simplicity, but this does not accurately describe the data hence using the non-linear form of the model is important.

2.6.1.2   Freundlich isotherm model

The Freundlich model was first used to describe adsorption of organic acids on coals by Freundlich (Freundlich, 1907).The Freundlich isotherm is used to account for the surface of the adsorbent being heterogeneous (Muedi *et al*, 2021). The adsorbent surface is assumed to be heterogenous, and the energy of active sites is exponentially described. It is therefore mainly applied to multi-layer adsorptions (Ma *et al*, 2014). The non-linearized form of the Freundlich isotherm model is expressed by Equation (2-4):

$$Q_e = K_F(T)C_e^{1/n_F} \tag{2-4}$$

Where K_F and n_F are the Freundlich isotherm parameters related to adsorption capacity (mg/g) and intensity of adsorption respectively. The adsorption intensity parameter (n_F) indicates how favourable an adsorption is, with values $n_F > 1$ indicating a favourable adsorption, , $n_F = 1$ linear adsorption and $n_F < 1$ unfavourable adsorption (Muedi *et al*, 2021). According to (Isiuku *et al*, 2021) a good adsorption process is indicated by values between 1 and 10. The linear form of Freundlich isotherm model is given by Equation (2-5*)*:

$$\ln Q_e = \ln K_F + \frac{1}{n} C_e \tag{2-5}$$

2.6.1.3   Multiple surface Langmuir isotherm model

According to McConnell *et al* (2020), neither Langmuir nor Freundlich isotherm models account for multiple pathways/surfaces of adsorption. This leads to underestimation of adsorption as well as reduction in the fit accuracy. The multiple surface Langmuir isotherm model was developed in 1918 by Irving Langmuir in his seminal work on adsorption modelling (Langmuir, 1918). The model assumes that there are multiple surfaces on which adsorption occurs thus improving the fit of adsorption compared to the general Langmuir and Freundlich models. The two-surface Langmuir isotherm is given by Equation (2-6):

$$Q_e = \frac{k_{L,1}(T)Q_{max,1}C_e}{1 + k_{L,1}(T)C_e} + \frac{k_{L,2}(T)Q_{max,2}C_e}{1 + k_{L,2}(T)C_e} \tag{2-6}$$

Where $K_{L,1}$, $K_{L,2}$ are the Langmuir adsorption equilibrium constant (L/mg) on the first and second surface and $Q_{max,1}$, $Q_{max,2}$ are the maximum adsorption capacity (mg/g) on the first and second surface respectively.

2.6.2 Adsorption thermodynamics

Thermodynamic parameters are very important when it comes to checking the feasibility as well as the spontaneity of adsorption process (Raghav and Kumar, 2018). Thermodynamic parameters of adsorption which include: the standard Gibbs free energy change (ΔG°), standard enthalpy change of adsorption (ΔH°), and the standard entropy change of adsorption (ΔS°) can be determined from Equation (2-7) (Tran, 2016):

$$\begin{cases} \Delta G°\text{=-RT}\ln(K) = \Delta H° - T\Delta S° \\ \therefore \ln(K) = -\dfrac{\Delta H°}{RT} + \dfrac{\Delta S°}{R} \end{cases} \tag{2-7}$$

Where K is the dimensionless equilibrium constant obtained from Langmuir isotherm model, R (J/mol/K) is the ideal gas constant and T (K) is the absolute temperature at which the isotherm was operated.

2.6.3 Adsorption kinetics

Kinetics of the adsorbent are studied in order to determine the residence time required for completion of the adsorption process (Kajjumba *et al*, 2018). This information is important for large-scale application of material. Mathematical models know as kinetic models are used to describe adsorption data (Manjuladevi *et al*, 2018). There are many kinetic models, but the most commonly used ones are the pseudo first-order (PFO) and pseudo second-order (PSO) models and their improvements.

2.6.3.1 Pseudo first-order kinetic model

The PFO model was developed by Lagergren (Lagergren, 1898). It assumes that a single (mono) layer is formed on the surface of the adsorbent. Even though this model is widely used it has many drawbacks which make its application and interpretation of the fitted results difficult. The fitted rate constant depends on initial concentration of the pollutant in the experiment hence the model cannot be applied in cases where the initial concentration is unknown thus limiting the application to batch systems only (Muedi *et al*, 2021). The model is described by Equation (*2-8*) below:

$$\frac{dQ}{dt} = k_1(Q_e - Q_t) \therefore Q_t = Q_e\left(1 - e^{-k_1 t}\right) \tag{2-8}$$

Where $k_1(\text{min}^{-1})$ is the first-order rate constant and Q_t (mg/g) is the amount adsorbed per unit mass at any time.

2.6.3.2 Pseudo second-order kinetic model

Pseudo-second -order model was first used in the 80s but it was after a study by Ho and McKay (Ho and McKay, 1999) that it became popular and has since been applied in different adsorption studies. The PSO model assumes a second-order dependence of the adsorbed amount on the available active sites. The model is described by the following equation:

$$\frac{dQ_t}{dt} = k_2(Q_e - Q_t)^2 \therefore Q_t = \frac{k_2 Q_e^2 t}{1 + k_2 Q_e t} \tag{2-9}$$

Where k_2 (g/mg min^{-1}) is the pseudo-second-order rate constant and is an indicator of how fast the reaction reaches the equilibrium. According to George William *et al* (2018), $Q_e - Q_t$ is the driving force and is proportional to the number of active sites available on the adsorbent.

2.6.3.3 *Two-phase adsorption kinetic model*

The two-phase adsorption (TPA) mostly known as two-compartment kinetic model was developed for temperature depended slow adsorption of organic compounds (Cornelissen *et al*, 1997). The TPA model was derived based on two parallel adsorption processes, a rapid and slow adsorption mechanism. According to Muedi *et al* (2021) the model provides an improvement to PFO and PSO models, however, the value of Q_e is not certain and this makes extrapolation of the model difficult.

$$\begin{cases} \dfrac{dQ_{t,fast}}{dt} = k_{fast}(Q_{e,fast} - Q_{t,fast}), \\ \dfrac{dQ_{t,slow}}{dt} = k_{slow}(Q_{e,slow} - Q_{t,slow}) \\ \qquad Q_{t,fast} + Q_{t,slow} = Q_t \\ \qquad Q_{e,fast} + Q_{e,slow} = Q_e \end{cases} \qquad (2\text{-}10)$$
$$\therefore Q_t = Q_{e,fast}(1 - e^{-k_{fast}t}) + (Q_e - Q_{e,fast})(1 - e^{-k_{slow}t})$$

Where k_1 (1/min), k_2 (g/(mg.min)),. k_{fast} (1/min), k_{slow} (1/min) are the pseudo first-order, second-order, fast, and slow rate constants, respectively. $Q_{t,fast}$ and $Q_{t,slow}$ represent the adsorbed amounts (mg/g) in the fast and slow adsorption phases, respectively, and $Q_{e,fast}$ and $Q_{e,slow}$ represent the equilibrium adsorbed amounts (mg/g) in the fast and slow adsorption phases, respectively.

2.7 Conventional materials used in adsorption

Presently different adsorbents have been used in the removal of Cr (VI) from water and wastewaters. These include graphene oxide and its composites, metal and metal oxides, carbon materials such as activated carbon, carbon nano-tubes.

2.7.1 *Graphene oxide and its composites*

Graphene oxide (GO) has drawn a lot of attention recently due to its lamellar shape and abundance of oxygen-containing groups such as carboxyl, hydroxyl and epoxy groups on its surface (Hou *et al*, 2021). Due to the characteristics mentioned above and its large surface area, GO has been used as an adsorbent sometimes after being combined with other materials. However, recycling the material is difficult because of the additional time-consuming centrifuging and filtration needed to separate the GO from the solution after usage (Hou *et al*, 2021). Magnetic adsorbents have therefore been used in combination with GO in order to overcome this challenge.

2.7.2 *Activated carbon*

Activated carbon is defined to include a large variety of amorphous carbon-based materials prepared through different methods such as physico-chemical treatment method (Roy and Halder, 2017),

hydrothermal carbonization (Liu *et al*, 2020) and recently microwave assisted production method (Ao *et al*, 2018).

Although activated carbon is safe and environmentally friendly, its pore sizes range between 0.4-4nm. This makes it inefficient in removing metals with small sizes (Gu and Yushin, 2014). Additionally, activated carbon has a low adsorption capacity, slow adsorption rate, as well as difficulties in separation and regeneration (Guo *et al*, 2022; Nowruzi *et al*, 2020).

In an effort to overcome the challenges associated with activated carbon materials, modification techniques have been applied in the production of activated carbon in the past. However these modifications can be cost intensive making the material costly to produce and they could lead to secondary pollution (Guo *et al*, 2022). Activated carbon is therefore mainly used as a support matrix to increase surface area of other materials. According to (Karimi-Maleh *et al*, 2021), removal by adsorption of Cr(VI) by activated carbon depends on the pre-treatment and activation method used. Activation can be used to incorporate functional groups and alter the surface chemistry of the activated carbon. This can boost the reduction of Cr(VI) to the less toxic Cr(III) by donation of lone pair of electrons during adsorption.

2.7.3 *Polyaniline*

In an effort to come up with cheaper and more effective materials for adsorption of heavy metals, recent studies have been exploring natural polymers and their composites. Among these cyclodextrin (Chen *et al*, 2022; El-Kafrawy *et al*, 2017; Verma *et al*, 2022), chitosan (Amin *et al*, 2023; Bakar *et al*, 2023; Xu *et al*, 2022b), starch and derivatives of starch (Ibrahim and Fakhre, 2019; Karić *et al*, 2023; Singh *et al*, 2020) and polysaccharides (Al-Dhabi *et al*, 2020; Zhang *et al*, 2023; Zhao *et al*, 2023) have received special attention. This is due to their ability to chelate heavy metals, their chemical stability, physical and chemical properties, and their unique structures (Abdel-Halim and Al-Deyab, 2011).

Electrically conducting polymers such as polyaniline (PANI) (Figure 2-3), polythiophene and polypyrrole have gained interest in removal of heavy metals owing to the many advantages associated with using them including low cost and ease of synthesis, environmental stability, ease of operation and regeneration and a high amine group content in their structure which adsorbs and chelates heavy metals via hydrogen bonding or electrostatic interactions (Jiang *et al*, 2018; Kera *et al*, 2017; Singh and Shukla, 2020). These polymers have many applications including drug delivery, chemical sensors, gas separation membranes, microwave adsorption, anti-corrosion coating among others (Jaymand, 2013; Lu *et al*, 2011). Due to its semiconducting and macromolecule nature owing to expanded pi bonding system, PANI is one of the most important conducting polymers. It is the second most widely used after polypyrrole. PANI is perfect for Cr(VI) removal due to its ability to simultaneously act as electron donor for the reduction of Cr(VI) to less harmful Cr(III) while also providing sites for adsorption of Cr(VI) (Harijan and Chandra, 2016; Kera *et al*, 2017).

According to Yuan *et al* (2018), there are two main methods used in the synthesizing of polymers such as PANI. These are electrochemical polymerization and chemical oxidative polymerization methods.

17

The latter includes simple methods such as dilute polymerization, in interfacial polymerization and rapidly mixed polymerization. The method used in polymerization of PANI as well as the conditions affect its morphology and hence its effectiveness. A study done by Bhadra *et al* (2007) showed that PANI synthesized via the electrochemical method had more a higher solubility, more benzenoid rings than quinoid rings, higher particle size and higher band energy compared to PANI synthesized by the chemical oxidative method.

In order to improve the structure, effectiveness and conducting ability of polymers, some chemicals can be used in a process known as doping. A chemical dopant is a material that, when added in relatively tiny amounts, significantly alters the electrical, optical, magnetic, and/or structural characteristics of the polymer and significantly increases conductivity (MacDiarmid and Epstein, 1995). According to MacDiarmid and Epstein (1995), there are two forms of doping. Redox doping involves the use of oxidizing or reducing agents to remove or add electrons to or from the polymer backbone. On the other hand, in acid/base (protonic acid) doping the number of electrons on the polymer remain unchanged.

Basic structure of Polyaniline
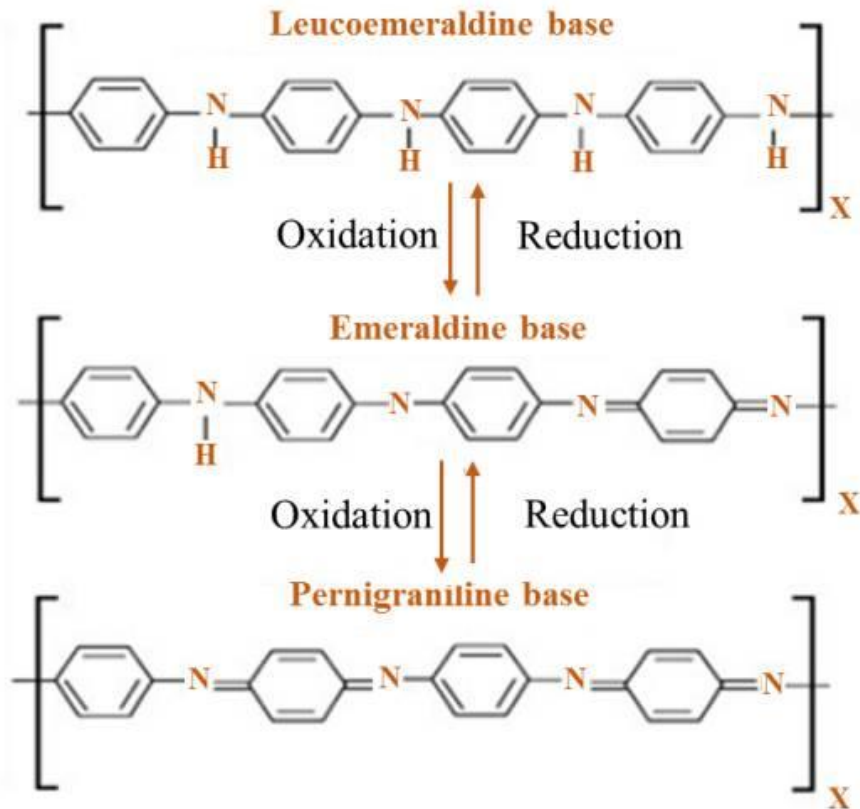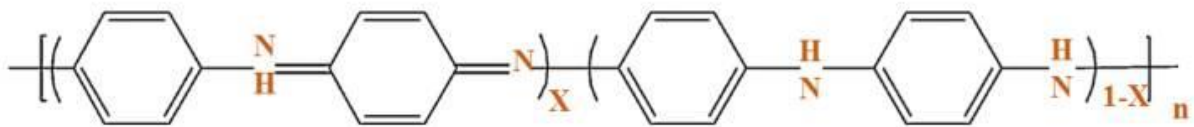
Figure 2-3: Basic chemical structure of PANI and its different bases (Beygisangchin *et al*, 2021).

2.8 Modern materials used for adsorption

Because of the limitations associated with conventional adsorption methods, many countries including South Africa are exploring the application of nanotechnology in water treatment. Nano-technology makes use of nanometre materials i.e. materials in the size 1-100 nm range. Owing to their increased specific surface area and small intraparticle diffusion distance nano-adsorbents have gained extensive applications in place of conventional adsorbents. Nano-adsorbents have been found to be effective in removal of heavy metals ions and their selectivity towards a particular pollutant can be increased by functionalization. Nanotechnology is thus a promising route to develop low-cost and high performance large scale plants for heavy metal removal.

2.8.1 Nanoparticles

In comparison to other materials used for adsorption over the years, nanoparticles have shown very high performance in the removal of metals from wastewater and have been successfully used in remediation technology (Noli *et al*, 2023). This is due to their tiny size hence a large surface area. Some of these

19

nanoparticles used in adsorption include copper based nanoparticles (Noli *et al*, 2023), nickel ferrite nanoparticles (Alamier *et al*, 2023), iron based nanoparticles e.g zero-valent iron (Bampaiti *et al*, 2013) among others. Despite their high performance, nanoparticles have limitations such as agglomeration which leads to decrease in surface area and high cost of synthesis.

Magnetic nanoparticles are being used to produce composites of polymers because magnetic separation via application of an external magnetic field can be used to overcome the challenge of separation and the process is easier than filtration and centrifugation (Kera *et al*, 2017). According to Gupta *et al* (2017), ferrites of general formula A-Fe_2O_4 e.g. $NiFe_2O_4$, $CoFe_2O_4$, $MnFe_2O_4$ and $CuFe_2O_4$ have been applied in many areas such as in microwave devices, gas sensor, colour imaging, electronic devices, ferro fluids, magnetic drug delivery, among others. This is due to their high specific heat capacity, high electrical selectivity, low melting point and high resistance to corrosion (Shanmugavel *et al*, 2014), (Gupta *et al*, 2017). Due to their special magnetic and chemical stability advantages, inorganic spinel ferrites and their composite materials have been employed extensively in water treatment among the existing magnetic sorbents. Nonetheless, the most significant type of is spinel nickel ferrite ($NiFe_2O_4$). This is because of its ferromagnetic properties which result from the spins of Fe^{3+} ions on the tetrahedral points and both the Ni^{2+} and Fe^{3+} ions on the octahedral points aligned in a parallel manner (Lingamdinne *et al*, 2016).

2.8.2   *Composites of polymer and nanoparticles*

Even though polymers have shown such a remarkable potential for the removal of heavy metals, when used on their own, these conducting polymers tend to have low adsorption capacity due to decreased surface area caused by agglomeration of particles. Additionally, it is a challenge to separate the polymer adsorbent from large volumes of solutions after adsorption (Das *et al*, 2019). This makes it hard to recover and recycle the adsorbent.

Even though (Agrawal and Singh, 2016) reported using $NiFe_2O_4$-PANI nanocomposite in a previous study, they reported a very low maximum adsorption capacity (12.19 mg/g). In this study, we investigate the effectiveness of 2-naphthalene sulfonic acid (2-NSA) doped polyaniline and nickel ferrite particle nanocomposite (PANI-NSA/$NiFe_2O_4$) produced via an in-situ chemical oxidative polymerization method in removing of Cr(VI) from aqueous solution.

Table 2-3: Nanocomposites used for removal of pollutants from wastewater.

Nanocomposite material	Target pollutant	Removal efficiency	Removal capacity (mg/g)	Reference
polyaniline@Ni(OH)$_2$	Cr(VI)	98 %	661.1	Bhaumik *et al* (2018)
Polypyrrole magnetite	Cr(VI)	99.2 %	208.77	Aigbe *et al* (2018)
Polypyrrole-polyethyleneimine	Pb	89.64 %	75.6	Birniwa *et al* (2022)
Fe$_3$O$_4$/ZnO/PANI	Congo red dye	81 %	96.46	Zare *et al* (2022)
PANI-CuO	Pb, Cd, Cr	79.9 %, 78.9 %, 82.1 % respectively	1.123, 1.409, 1.342	Kumar and Joshi (2022)
Graphene oxide/SiO$_2$/Polyaniline	Cu(II) and Cr(VI)	-	512.47 and 258.275	Kumar *et al* (2020)
Copper ferrite-polyaniline	Methyl orange dye	-	345.9	Kharazi *et al* (2019)
Polyaniline/Hexagonal Mesoporous Silica (PANI/HMS) nanocomposite	Ni(II)	100 %	253.17	Javadian *et al* (2013)
Magnetite-polyethyleneimine montmorillonite	Cr(VI)	84 %	8.77	Larraza *et al* (2012)
Polyaniline/ZnO	Methyl orange dye	99.5 %	47.62	Garg *et al* (2022)
Fe3O4 @Chitosan-Zr-PANI)	Cr(VI)	100 %	491.43	Xu *et al* (2022a)
Reduce graphene oxide/Fe$_3$O$_4$ − TiO$_2$	Malachite green dye	99 %	-	Bibi *et al* (2021)

Chapter 3   Materials and Methods

3.1 Chemical reagents and standards

Aniline (C_6H_7N), ammonium persulfate ($APS(NH_4)_2S_2O_8$), 2-Naphthalene sulfonic acid (2-NSA, $C_{10}H_8O_3S$), potassium dichromate ($K_2Cr_2O_7$), 1,5-diphenylcarbazide (DPC) and nickel ferrite ($NiFe_2O_4$) nanopowder (<50 nm particle size) were purchased from Sigma Aldrich. Sulphuric acid (H_2PO_4, 98 wt%), nitric acid (HNO_3, 98 wt%), sodium hydroxide (NaOH) and methanol (CH_3OH) were obtained from Fisher Scientific and Glassworld. All the chemicals were used as received without any further treatment.

3.2 Preparation of chromium stock solution

The Cr (VI) stock solution (1000 mg/L) of Cr (VI) was prepared by dissolving 1.414 g of potassium dichromate ($K_2Cr_2O_7$) in ultrapure water in 1000 mL volumetric flask. Fresh working solutions for each experiment were prepared from the stock solution.

3.3 Preparation of 1,5-DPC solution for Cr (VI) analysis

1,5-DPC solution was prepared by dissolving 125 mg of 1,5-DPC in 25 mL of methanol. 7 mL of H_2SO_4 (98%) was mixed with 125 mL deionized water and added to the above solution to make a 250 mL total volume.

3.4 Synthesis of PANI and PANI/NiFe$_2$O$_4$

PANI-NSA/ $NiFe_2O_4$ PNC was fabricated by emblematic in-situ oxidative polymerization method which was adapted from elsewhere (Long *et al*, 2005). In this synthesis method, 0.2 mL aniline and predetermined amount of $NiFe_2O_4$ nano-powder were mixed with 80 mL of 2-NSA solution (0.416 g of 2-NSA dissolved in 80 mL of deionized water) under ultrasonic agitation for 15 minutes. During the agitation period, aniline reacted with 2-NSA to form NSA-ANI micelles containing $NiFe_2O_4$ nano-powder. Thereafter, 0.456 g of APS dissolved in 5 mL of deionized water in a separate beaker was added to the above $NiFe_2O_4$ suspension and sonicated for another 1 minute. The mixture was labelled (PANI-NSA/$NiFe_2O_4$, wt%) and kept undisturbed under room temperature for 24 h for in-situ polymerization. After 24 hours the product was vacuum filtered and washed with deionized water. Further washing with methanol was done to remove any possible oligomers. The final PNC product was dried in vacuum oven at 60 °C for 24 h. The synthesis process is shown in Figure 3-1. Pure PANI was synthesized in the same manner without adding nickel ferrite.

3.5 Chromium analysis methods

A UV VIS spectrophotometer at 540 nm wavelength was used to determine the final concentration of Cr (VI) ions in the aqueous medium after adsorption. Standard solutions of 1 mg/L, 0.5 mg/L, 0.25 mg/L, and 0.1 mg/L of Cr (VI) were used for the instrument's calibration curve. Flame Atomic Absorption Spectrometer (FAAS) was used to determine the total chromium after adsorption. Standard solutions of 1 mg/L, 2.5 mg/L, and 5 mg/L were used for the FAAS calibration.
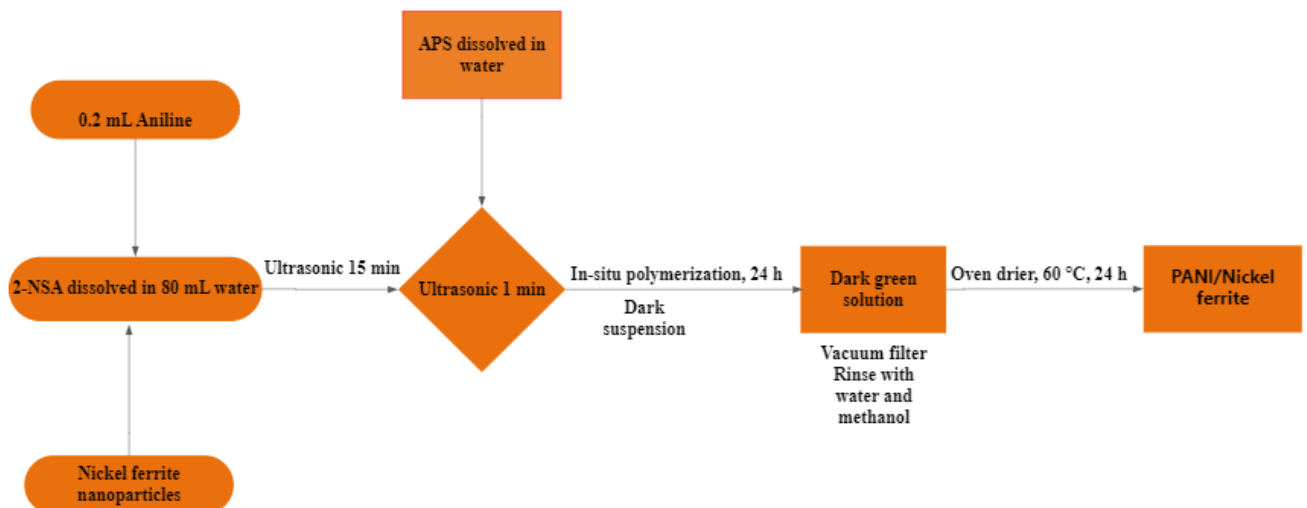
22

Figure 3-1: Synthesis process of PANI-NSA/NiFe$_2$O$_4$ nanocomposite

3.6 Preliminary studies

It was noted from literature (Aigbe *et al*, 2018; Samuel *et al*, 2018) that acidic pH values and especially pH 2 gave a better removal percentage of Cr (VI) from solution hence initial pH of 2 was chosen for the preliminary studies.

Preliminary studies were done to determine the optimum loading of NiFe$_2$O$_4$ in the PNC as well as the initial dosage for the batch experiments. To determine the optimum loading, the following masses of NiFe$_2$O$_4$ were used in the synthesis of the nanocomposite (10, 20, 25, 50, 100 mg). The obtained nanocomposites were used to remove 100 mg/L of Cr (VI) from 25 mL solution at pH 2. The solutions were shaken in the thermostatic water bath shaker at 25 °C with a shaking speed of 200 rpm. The initial pH of the solution was adjusted using HNO$_3$ (0.1 M) and/or NaOH (0.1 M).

It was observed that a loading of 10 mg of NiFe$_2$O$_4$ in the nanocomposite led to a 94.9% removal of Cr (VI) from the solution. Changing the loading of NiFe$_2$O$_4$ from 10 to 20 mg led to a very slight increase in the percentage removal of Cr (VI) (95.7%) while any further increase from 20 mg led to a decline in the percentage removal to 80.8% at 100 mg loading. Even though a higher loading of NiFe$_2$O$_4$ would increase the effectiveness of the material with reference to magnetic properties, the loading mass of 10 mg was used in the batch studies.

Initial studies to determine the optimum dose for batch experiments were done where the dose of PNC was varied from 5 mg to 40 mg while the solution pH, the initial Cr (VI) concentration and the sample volume were kept constant at 2, 25 mg/L, and 25 mL, respectively. It was observed that complete removal of Cr (VI) was observed for all the dosages and therefore for the batch experiment, the initial Cr (VI) concentration and sample volume were both increased to 50 mg/L and 50 mL respectively.

3.7 Batch adsorption studies

All effect of initial Cr (VI) concentration, effect of temperature, effect of dosage and initial Cr (VI) pH effect experiments were conducted in a thermostatic water bath shaker agitated at 200 rpm for 24 hours

23

using 100 mL glass bottles containing 50 mL solutions of Cr (VI). Effect of agitation time experiments were conducted using an overhead stirrer on a 1000 mL beaker filled with 500 mL solutions of Cr (VI) mixed at a speed of approximately 200 rpm. All experiments were carried out twice and the average value reported.

3.7.1   Effect of dosage

To test effect of PANI-NSA/ $NiFe_2O_4$ dosage, Cr (VI) solutions were contacted with PANI-NSA/ $NiFe_2O_4$ nanocomposite whose dose was varied between 5 and 40 mg. The different masses of the adsorbent were weighed using a 4-decimal point digital mass balance. The efficiency (% removal) of Cr (VI) was calculated using Equation (3-1):

$$\% \text{ removal} = \frac{C_o - C_e}{C_o} \times 100 \tag{3-1}$$

where C_o and C_e are the initial and equilibrium concentration of Cr (VI), respectively, in mg/L.

3.7.2   Effect of solution pH

To analyze the effect of initial Cr (VI) solution pH on the removal of Cr (VI) by the synthesized PANI-NSA/ $NiFe_2O_4$, the initial pH of the Cr (VI) solutions was adjusted to pH values between 2 and 11 before contacting with 25 mg of PANI-NSA/ $NiFe_2O_4$ nanocomposite.

3.7.3   Point of zero charge

The point of zero charge (PZC) study was done following a method described elsewhere (Castellar-Ortega *et al*, 2019). 0.125 g of adsorbent was added in 25 mL deionized water into several sample bottles, later the pH was adjusted between 2 and 12 units with solutions of HCl 0.1 M and NaOH 0.1 M. After 24 h the final pH was measured.

3.7.4   Effect of initial concentration

To test the effects of initial concentration, Cr (VI) solutions with concentration varied between 50 and 400 mg/L were prepared from the stock solution. The equilibrium capacity was determined using Equation (3-2):

$$Q_e = \frac{C_o - C_e}{m} \times V \tag{3-2}$$

Where Q_e (mg/g) is the amount of Cr (VI) adsorbed per unit mass of adsorbent at equilibrium, m is the mass of the adsorbent (g) and V is the sample volume (L). To test the effect of temperature the effects of initial concentration experiment was carried out at 3 different temperatures (25 °C, 35 °C and 45 °C) in a thermostatic shaker. The results were used for isotherm modelling.Table *3-1* summarizes the conditions for isotherm experiments.

Table 3-1: summary of studied parameters for adsorption isotherms

Experiment	Temperature (°C)	Adsorbent dosage (mg)	Initial Cr (VI) concentration (mg/L)	Initial pH of Cr (VI) solution	Experimental time (hours)
1	25	25	50, 100, 150, 200, 250, 300, 350, 400	2 ± 0.03	24
2	35	25	50, 100, 150, 200, 250, 300, 350, 400	2 ± 0.03	24
3	45	25	50, 100, 150, 200, 250, 300, 350,400	2 ± 0.03	24

3.7.5   Effect of contact time

The effect of contact time was studied by contacting 500 mL Cr(VI) of solution with 150 mg of PANI/ $NiFe_2O_4$ nanocomposite in a beaker continuously stirred at 200 rpm with a non-magnetic stirrer. Three initial Cr(VI) concentration (50, 100 and 200 mg/L) were studied over a 6 h period. Sample volumes of 4 mL were drawn from the beaker in selected time intervals between 0 and 360 min and analysed for residue Cr (VI) and Cr(III) concentration. The adsorption capacity of the adsorbent, Q_t (mg/g) at any time was obtained from Equation (3-3):

$$Q_t = \frac{C_o - C_t}{m} \times V \tag{3-3}$$

Where C_t (mg/L) is Cr (VI) concentration in the solution at any time t. The results obtained from this experiment were used for kinetic model fitting.

3.7.6   Effect of other ions

To test the effect of co-existing ions on the adsorption of Cr (VI), copper (Cu^{2+}), zinc (Zn^{2+}), sulfate (SO_4^{2-}), and nitrate (NO_3^-) ions were used in a mixed (binary) sorption system described by (Bhaumik *et al*, 2018). In this experiment, 50 mL aqueous solution containing initial concentration of 50 mg/L of Cr (VI) and initial concentrations of the co-existing ions (50, 100, 150 mg/L) was mixed with 0.025 g of PANI/NiFe$_2$O$_4$ and shaken at room temperature for 24 h after which it was analysed for Cr (VI) concentration.

3.7.7   Desorption studies and re-usability

To test the regeneration of PANI-NSA/NiFe$_2$O$_4$, 0.05 g of PANI-NSA/NiFe$_2$O$_4$ was conducted with 50 mL of 50 mg/L Cr (VI) solution in a 100 mL glass bottle. After 24 h, a centrifuge was used to separate the solid material residual from the supernatant. The supernatant was analysed for Cr (VI).
 The residual was washed with de-ionized water to remove excess Cr (VI) and mixed with 50 mL of 1M NaOH and sonicated for 5 minutes. The Cr (III) concentration was calculated from the difference between the total chromium and Cr (VI) concentration. The same desorption step was repeated with HNO$_3$ to remove Cr (VI) ions. The residue recovered from the two desorption steps was mixed with

de-ionized water and centrifuged for 25 min at 9000 rpm before separating. It was then contacted with a new Cr (VI) solution for a new adsorption cycle.

3.7.8 *Test on real chromium water*

Chromium wastewater from a chrome plating company in Silverton (Pretoria), South Africa was used for this study. After measuring the initial concentration of Cr (VI) in the wastewater, it was diluted to a 50 mg/L concentration using de-ionized water. 50 mL of the solution were contacted with varying doses of PANI-NSA/$NiFe_2O_4$ (15, 25, 30 and 40 mg) after adjusting the pH to 2. The solutions were shaken for 24 hours after which the final Cr (VI) concentration was measured.

3.8 Characterization

A Micrometrics TriStar II BET analyzer (Micrometrics Inc., Norcross, GA) was used to obtain the 124 Brunauer-Emmett-Teller (BET) specific surface area and pore size of PANI-NSA and PANI-NSA/$NiFe_2O_4$ nanocomposite. Liquid nitrogen at 77 K was used for the measurement. To remove impurities and moisture from the samples before analysis, degassing was done by vacuum drying for 10 h at a temperature of 100 °C. A field emission scanning electron microscope (Zeiss Ultra PLUS FEG SEM) and a high resolution transmission electron microscope (Jeol 2100F FEG TEM) were used to obtain morphological images of PANI-NSA and PANI-NSA/$NiFe_2O_4$ and Energy Dispersive X-Ray (EDX) composition analysis of PANI-NSA/$NiFe_2O_4$. The morphology of the material was checked on the material as synthesized without coating. X-ray photoelectron spectroscopy (XPS) was used to characterize the PANI-NSA/$NiFe_2O_4$ before and after Cr (VI) adsorption with a Thermo ESCAlab 250 Xi (USA). The samples were washed with water and methanol and dried at 60 °C after adsorption. Silica gel was placed in the container with the samples to remove moisture. Functional groups of the PANI-NSA/ $NiFe_2O_4$ nanocomposite were obtained from IR spectra using a Perkin-Elmer (USA) Fourier transform infrared spectrometer (Spectrum 750 S spectrometer). To explore the temperature dependent magnetic properties of the composite and its components, a Physical Property Measurement System (PPMS) from Quantum Design (USA) with a Vibrating Sample Magnetometer (VSM) measurement mode was used. X-ray diffraction (XRD) crystalline profiles for $NiFe_2O_4$ and PANI-NSA/$NiFe_2O_4$ were recorded on a PANanalytical X'pert PRO diffractometer.

Chapter 4   Results and discussions

4.1 Characterization

BET results indicated that the surface area of PANI-NSA/ $NiFe_2O_4$ (26.513 $\frac{m^2}{g}$) is higher than that of PANI-NSA (21.773 $\frac{m^2}{g}$) which shows that synthesizing a composite of PANI and $NiFe_2O_4$ significantly increases the surface area of the material. SEM images of synthesized pure PANI-NSA and PANI-NSA/ $NiFe_2O_4$ are shown in Figure 4-1 (a) and Figure 4-1 (b).

(a)   (b)

(c)   (d)
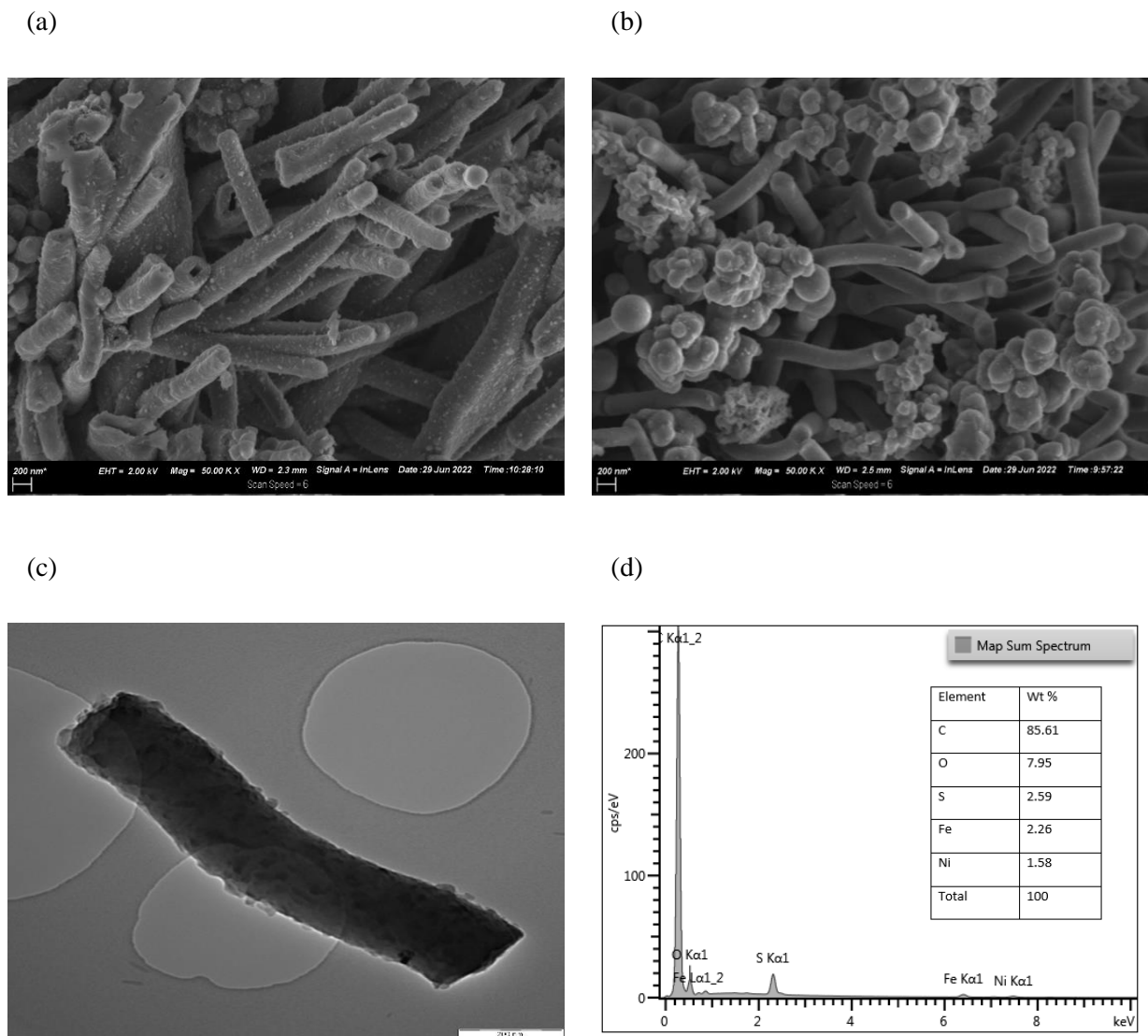
Figure 4-1: SEM images of (a) PANI-NSA/ $NiFe_2O_4$, (b) PANI-NSA (b) and (c) TEM image of PANI-NSA/ $NiFe_2O_4$ and (d) EDX analysis of PANI-NSA/ $NiFe_2O_4$.

From the images (Figure 4-1 (a) and Figure 4-1 (b)), it can be observed that PANI-NSA forms rod-like structures whose surface is smooth while PANI-NSA/ $NiFe_2O_4$ composite forms rods with a rough surface. The rough surface is linked to $NiFe_2O_4$ attaching on to the forming PANI-NSA. This increases

27

the pore diameter and provides more surface for Cr (VI) adsorption. It is also observed that PANI-NSA exhibits noticeable agglomeration while PANI-NSA/ NiFe$_2$O$_4$ has less agglomeration with most rods occurring individually (Figure 4-1 (a) and Figure 4-1 (b)). Figure 4-1 (c) shows the TEM analysis of PANI-NSA/NiFe$_2$O$_4$. It can be noted that the NiFe$_2$O$_4$ nanoparticles are completely encapsulated in the PANI-NSA/NiFe$_2$O$_4$ structure (signified by the presence of dark spots). This confirms that this method allows for the encapsulation of NiFe$_2$O$_4$ in the forming rods of aniline during the polymerization. A study by Bhaumik et al (Bhaumik *et al*, 2019) yielded similar results. The EDX analysis shown in Figure 4-1 (d) confirms the presence of Ni and Fe ions in the structure of the PANI-NSA/NiFe$_2$O$_4$. The EDX results also show that the polymer (PANI-NSA) is the main component of the PANI-NSA/NiFe$_2$O$_4$ due to the higher composition of C and H.

The species of PANI-NSA/NiFe$_2$O$_4$ as well as the valence of chromium on the surface of PANI-NSA/NiFe$_2$O$_4$ were determined by XPS. The results obtained from XPS before and after treatment with Cr (VI) solution are shown in Figure 4-2(a). C1s, N1s, O1s, S2ps are observed at the corresponding binding energies of 284.9, 399.3, 531.8, 168.2 eV suggesting presence of mainly PANI in the PANI-NSA/ NiFe$_2$O$_4$ nanocomposite. Additionally, Cr2p peak was observed at 577.3 eV in the after treatment XPS spectrum as shown in Figure 4-2(b) confirming the adsorption of Cr (VI) on the surface of the PANI-NSA/NiFe$_2$O$_4$ nanocomposite.

No peaks suggested the presence of NiFe$_2$O$_4$ on the surface of the nanocomposite. This could be due to the low composition of NiFe$_2$O$_4$ in the nanocomposite. Another possible explanation is that since XPS is a surface method of analysis, it may not detect the Ni and Fe ions since NiFe$_2$O$_4$ is encapsulated in the PANI-NSA structure. The presence of S2p peaks in the nanocomposite indicates presence of sulfur group due to the doping of PANI with NSA. The deconvoluted S2p peaks Figure 4-2(b) shows that the of SO_3^{2-} group which was present before treatment with Cr (VI) solution (Figure 4-2(a)) disappears after treatment with Cr (VI) solution indicating that SO_3^{2-} group takes part in the removal of chromium. The N1s spectrum in the PANI-NSA/NiFe$_2$O$_4$ before treatment with Cr(VI) solution was deconvoluted into 2 distinct curves with peaks at 399.2 and 400.7 (Figure 4-2(c,d)) while two curves with peaks at 399.3 and 401.2 are observed in the PANI-NSA/ NiFe$_2$O$_4$ after treatment with Cr(VI) solution (Figure 4-2(e,f)). The peaks at 399.2 and 399.3 are related to the undoped amine groups (-NH-) while the peaks at 400.7 and 401.2 are related to the doped amine (-NH$^+$) and (-NH$_4^+$) cations associated with the ammonium persulfate used in oxidation of aniline in the polymerization process.
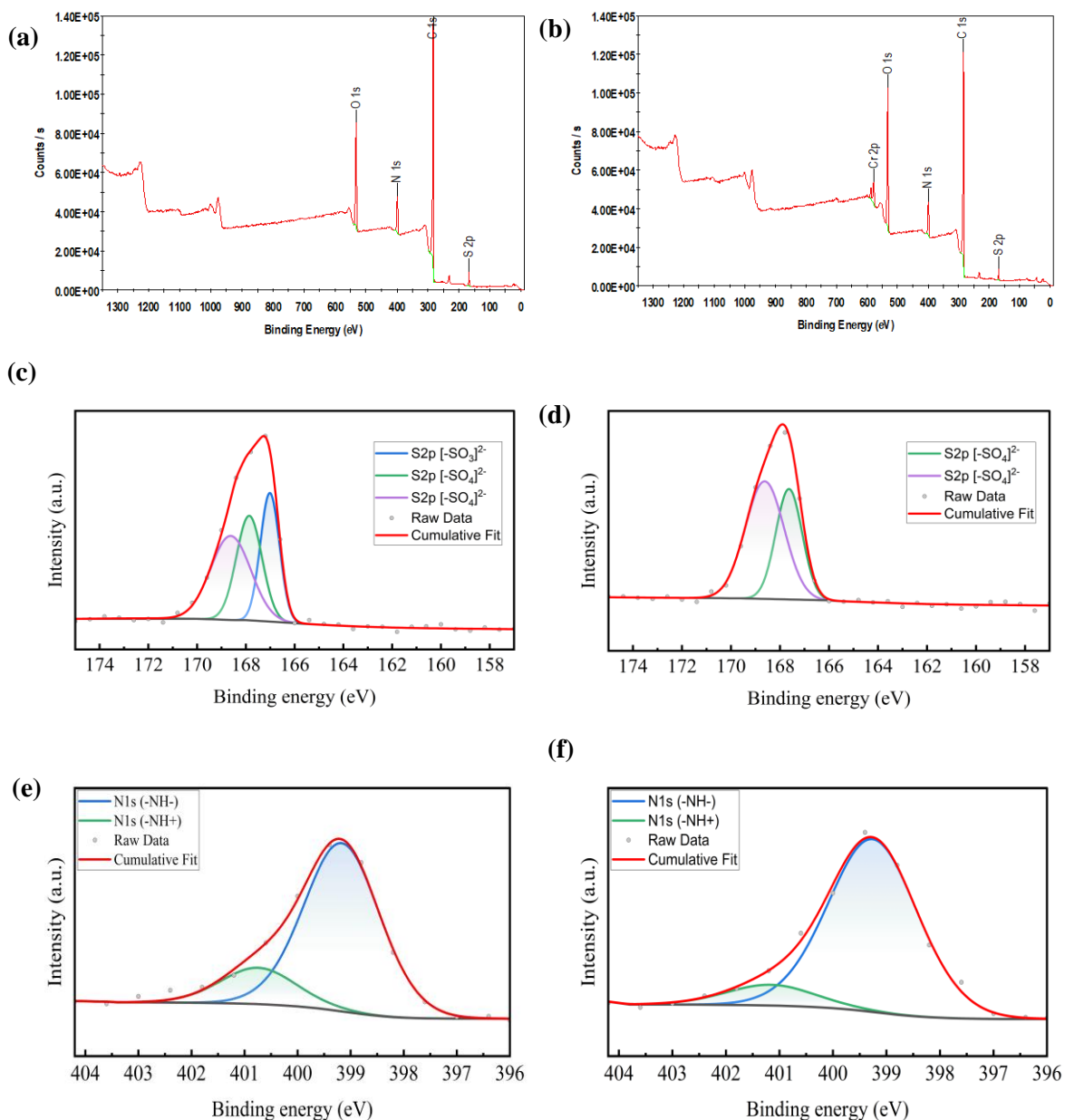
Figure 4-2: XPS survey of PANI-NSA/ Ni Fe$_2$O$_4$ (a) before and (b) after treatment with Cr (VI) and deconvoluted peaks of before and after treatment with Cr (VI) for: (c, d) S2ps, (e, f) N1s.

The FTIR spectra of PANI-NSA/ NiFe$_2$O$_4$ nanocomposite, NiFe$_2$O$_4$ nanoparticles and PANI are shown in

Figure 4-3. Peaks of PANI-NSA are observed at 1575, 1488, 1299, 1238, 1048, 1028, 829, and 670 cm^{-1}. The peaks at 1575 and 1488 are associated with functional groups of C-C bond of quinonoid and benzenoid rings, peak at 1299 associated with C-N stretching of the B rings as a result of protonation of PANI (Basavaraja *et al*, 2014). The peak at 1238 represents –C(CO)O- stretching (Terraza *et al*, 2018), at 1048 the presence of C-O stretching (Lingegowda *et al*, 2012), and the peak at 829 is

29

associated with C-H bonds in aromatic rings, peaks at 1028 and 670 are associated with doped -SO_3H group (Macherla *et al*, 2022).
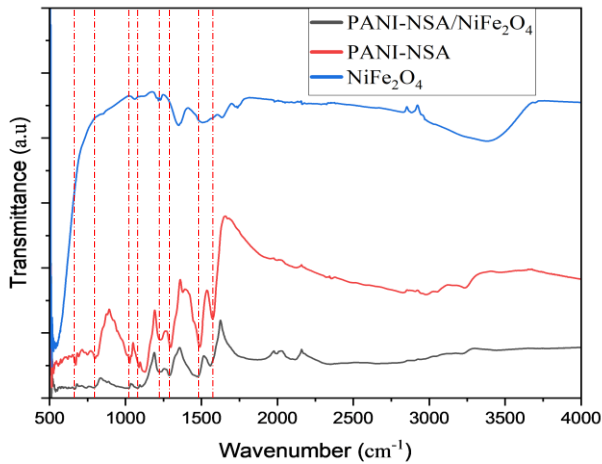
Figure 4-3: FTIR spectrum of PANI-NSA, Ni Fe_2O_4 and PANI-NSA/ Ni Fe_2O_4 composite.

Figure 4-4 depicts the magnetic hysteresis loops of PANI-NSA, Ni Fe_2O_4, and PANI-NSA/Ni Fe_2O_4 composite. According to the graph, the magnetization of PANI-NSA/Ni Fe_2O_4 and Ni Fe_2O_4 increased and tended to reach saturation as the magnetic field increased. The magnetization values are 25 and 2.5 emu/g for Ni Fe_2O_4 and PANI-NSA/Ni Fe_2O_4 respectively. As a result, the magnetization curves shows that the PANI-NSA/Ni Fe_2O_4 composite has good magnetic properties.
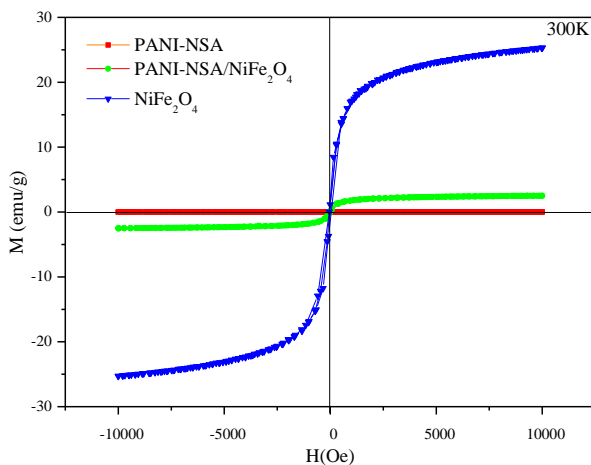
Figure 4-4: Magnetic hysteresis loops of PANI-NSA, Ni Fe_2O_4, and PANI-NSA/Ni Fe_2O_4 composite

30

Figure 4-5 gives the XRD pattern of $NiFe_2O_4$ and $PANI-NSA/NiFe_2O_4$ nanocomposite. The diffraction peaks observed at 2θ of 21.7° (111), 35.8° (220), 41.8° (311), 43.3° (222), 51.3° (400), 63.5° (422), 67.5° (511) and 75.0° (440) are the characteristic peaks of $NiFe_2O_4$ (PDF Card 96-591-0065). The characteristic peaks are also observed on the $PANI-NSA/NiFe_2O_4$ nanocomposite XRD pattern even though they broaden out. This confirms the interaction between PANI-NSA and $NiFe_2O_4$ in the formation of $PANI-NSA/NiFe_2O_4$ nanocomposite. Additionally, these broader peaks could be due to $NiFe_2O_4$ nanoparticles being covered by PANI-NSA.
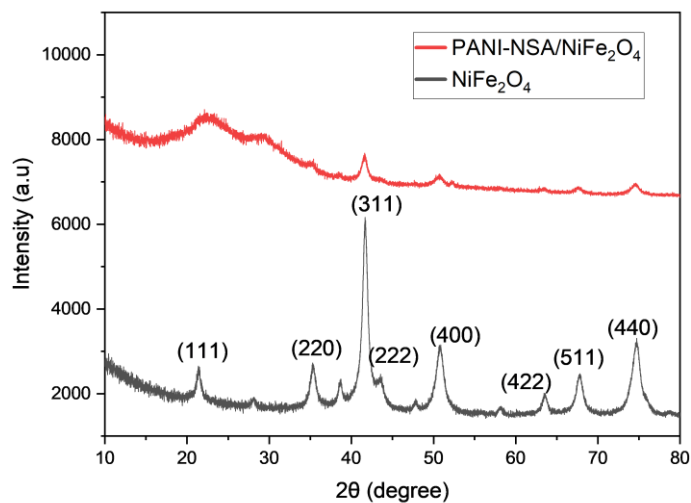
Figure 4-5: XRD pattern of $PANI-NSA/Ni Fe_2O_4$ and $Ni Fe_2O_4$

4.2 Effect of solution pH

Solution pH has an effect on the Cr (VI) removal efficiency because it determines the charge on the surface of the adsorbent as well as the degree of ionization and speciation of the adsorbate which affects the ions available in the aqueous solutions (Agrawal and Singh, 2016). Figure 4-6 (a) shows the effect of initial solution pH on the removal efficiency of Cr (VI) by $PANI-NSA/Ni Fe_2O_4$. It is observed that the percentage removal of Cr (VI) by $PANI-NSA/Ni Fe_2O_4$ decreases with an increase in the pH of the solution with the maximum removal observed at pH 1 and 2. The pH dependence of Cr (VI) removal rate by $PANI-NSA/Ni Fe_2O_4$ is due to the existence of different chromium species at different pH values and change in the charge of the $PANI-NSA/ Ni Fe_2O_4$ surface which affect the adsorption efficiency. In acidic solution conditions (pH values between 1 and 6), $HCrO_4^-$ predominantly coexists with $Cr_2O_7^{2-}$ while at higher pH values (pH values above 6), $Cr_2O_7^{2-}$ is the predominant species. Additionally, in acidic conditions, the surface of $PANI-NSA/Ni Fe_2O_4$ is highly protonated due to the presence of NH^+ functional groups. This leads to a high electrostatic attraction between the oxyanions of Cr (VI) and the positively charged surface of the adsorbent. As the pH increases, the positive charge on $PANI-NSA/Ni Fe_2O_4$ surface decreases and thus a decline in the removal rate due to the repelling

31

nature between the surface and the oxyanions. Additionally, at pH above 6 there is a high abundance of hydroxyl (OH^-) ions which compete with the oxyanions of Cr(VI) for the active sites thus leading to a further decrease in Cr (VI) removal. (Agrawal and Singh, 2016) and (Yang *et al*, 2014) reported a similar trend on the effect of pH on the Cr (VI) removal efficiency.

(a)   **(b)**

(c)
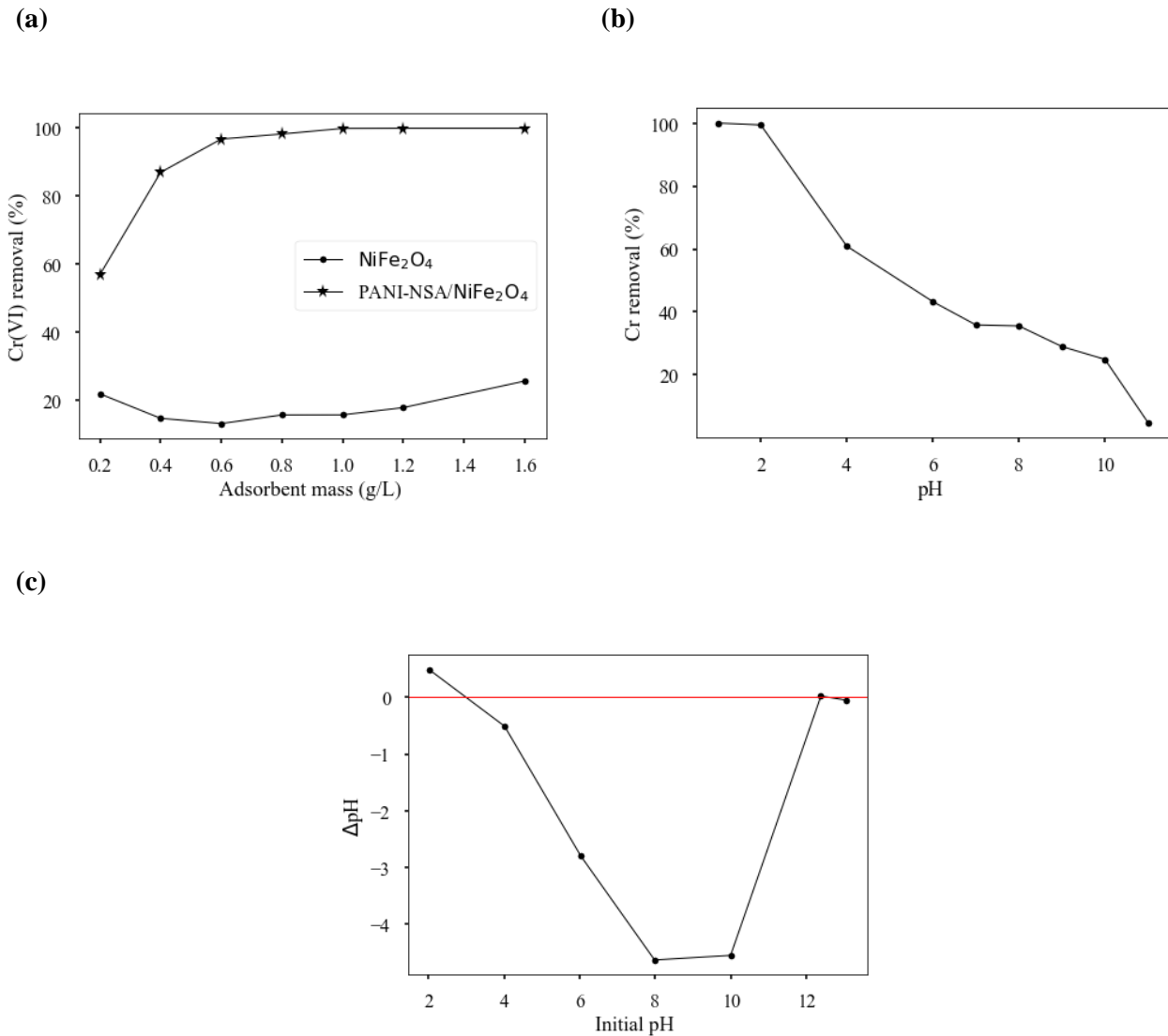
Figure 4-6: Effect of (a) dosage and (b) pH on Cr (VI) removal efficiency and (c) point of zero charge of PANI-NSA/NiFe$_2$O$_4$.

4.1 Determination of point of zero charge

The pH of the solution is important in cation adsorption because it effects the speciation and ionisation of adsorbent active sites (Hamadeen *et al*, 2022). The net charge of the adsorbent affects the protonation-deprotonation behaviour of the adsorbent which is relevant in explaining the mechanism of adsorption. The point of zero charge determines the charge on the surface of the adsorbent and hence the electrostatic interactions between the adsorbent and the adsorbate. At a solution pH equal to the point of zero charge pH (pHpzc), the adsorbent's surface charge is neutral. When the pH of the solution

is less than pHpzc, the adsorbent operates as a positively charged surface; whereas when it is greater than pHpzc, the adsorbent behaves as a negatively charged surface (Asanu *et al*, 2022). From Figure 4-6 (c), it is observed that the pHpzc of PANI-NSA/Ni Fe_2O_4 is 2.8 ± 0.1. This shows that PANI-NSA/Ni Fe_2O_4 surface is positively charged at pH below 2.8 which attracts the negatively charged $HCrO_4^-$ hence the higher Cr (VI) removal efficiency observed at lower pH values. At pH above 2.8, the surface of PANI-NSA/Ni Fe_2O_4 is negatively charged which repels the CrO_7^{2-} ions hence lower Cr (VI) removal efficiency. These results are consistent with the effect of pH results which show a rapid drop in the Cr (VI) removal efficiency when pH is increased from 2 to 4.

4.2 Effect of dose

Figure 4-6 (b) shows the effect of dose on the removal of Cr (VI) from the aqueous solution. It can be observed that the removal efficiency from a 50 mL of 50 mg/L Cr (VI) solution increases from 56.9% for 0.2 g/L adsorbent mass to 99.9% for 1 g/L adsorbent mass. This is due to an increase in surface area which translates to more active sites being available for adsorption. The removal percentage does not change with any further increase in adsorbent dose due to the adsorbate (Cr (VI)) becoming limiting in the system which means that the concentration of Cr (VI) is less than the active sites available for adsorption. This also shows that an adsorbent loading of 1 g/L is enough to remove Cr (VI) from 50 mL solution with an initial Cr (VI) concentration of 50 mg/L. These results were consistent with two other previous studies (Fan *et al*, 2017), (Bhaumik *et al*, 2018) and confirm that PANI-NSA/NiFe$_2$O$_4$ nanocomposite has a high affinity for Cr (VI) removal. In another study using a nickel ferrite-polyaniline material synthesized through oxidative polymerization, (Agrawal and Singh, 2016) found that an adsorbent dosage of 0.5g/10 mL attained a 70% removal of Cr(VI) from 10 mL of 10 mg/L initial Cr(VI) concentration which confirms that the PANI-NSA/NiFe$_2$O$_4$ synthesized in this study has a higher removal capacity. Comparing the performance of pure Ni Fe_2O_4 to that of the PANI-NSA/NiFe$_2$O$_4$ nanocomposite shows that pure PANI-NSA/Ni Fe_2O_4 nanocomposite performs better than pure Ni Fe_2O_4 implying that modifying the nanoparticles with PANI-NSA increases the surface area for adsorption.

4.3 Adsorption isotherms

Figure 4-7 (a) shows the effect of initial Cr (VI) concentration. It is observed that the percentage removal of Cr (VI) declines with increase in initial Cr (VI) concentration. This is due to enough active sites not being available for the adsorption. Since the number of active sites is not increasing, increasing the concentration of Cr (VI) does not lead to any significant increase in the Cr (VI) uptake. It was also observed that the percentage removal increases with increase in temperature signifying that the process is endothermic in nature. The maximum removal of Cr (VI) is observed at 45 °C for all concentrations hence this is the optimum temperature recommended for this process.

(a)

(b)

(c)

(d)
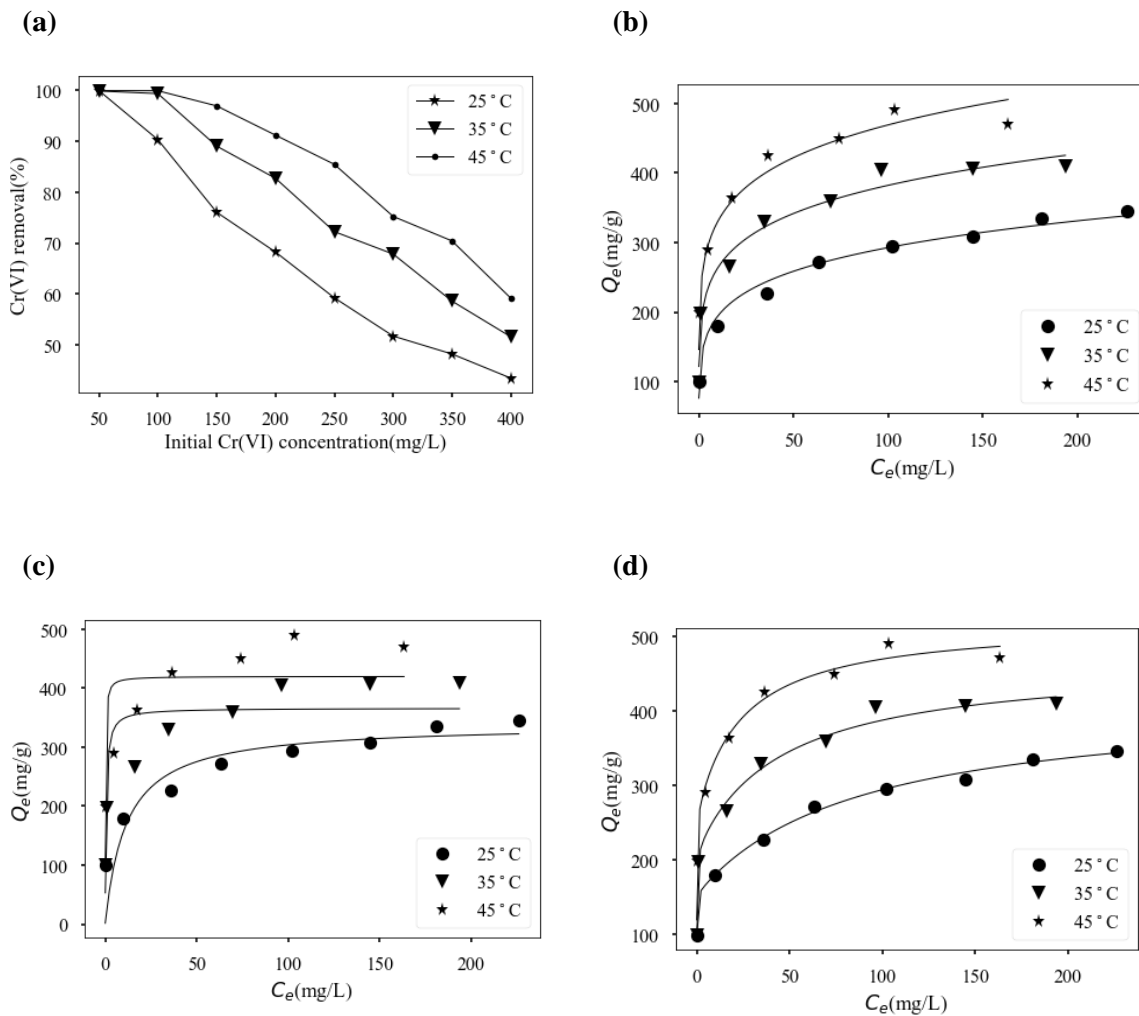
Figure 4-7: (a) Effect of initial concentration and (b) Freundlich, (c) Langmuir and (d)Two-surface Langmuir isotherm fitting.

Figure 4-7 (b, c, d) shows the fitting of non-linearized Langmuir, Freundlich and Two-surface Langmuir isotherm models on the experimental data at different temperatures. The increasing value of Q_e with an increase in temperature for all models confirms that the adsorption of Cr(VI) on PANI-NSA/ Ni Fe$_2$O$_4$ is an endothermic process. The various adsorption parameters calculated from these model fittings are given in Table 4-1. The coefficient of determination (R^2) is observed to decrease in the order: Two surface Langmuir, Freundlich and Langmuir indicating that the Two-surface Langmuir isotherm model best fits the isotherm data confirming that adsorption of Cr(VI) occurs on more than one surface sites. The observation that $K_{L2} \to \infty$ indicates that the second surface corresponds to irreversible adsorption, i.e. initially surface corresponding to K_{L2} and Q_{max2} (second surface) is saturated with irreversibly, after which the surface corresponding to K_{L1} and Q_{max1} (first surface) reversibly adsorbs the adsorbate. This results in $C_e = 0$ values for low initial concentrations of adsorbate, at higher initial concentrations the second surface saturates and the first surface starts to reversibly adsorb the adsorbate. It is noteworthy

34

that the first surface has a $Q_{max,1}$ which was nearly independent of temperature, while the second surface exhibited a significant increase in $Q_{max,2}$ for increased temperature.

The Freundlich isotherm second best describes the isotherm data in this study. The fitted parameter $n_F>1$ for all temperatures implying that adsorption is favourable at all the studied temperatures. For Langmuir isotherm model, the K_L values increased with an increase in temperature indicating an increased affinity for Cr(VI) by PANI-NSA/ Ni Fe$_2$O$_4$ with increase in temperature. The calculated Q_{max} values are comparatively higher when compared to that of other studies (Agrawal and Singh, 2016; Aigbe *et al*, 2018; Karthik and Meenakshi, 2014; Yang *et al*, 2014) which further confirms that the synthesized PANI-NSA/ Ni Fe$_2$O$_4$ has a very high affinity for Cr (VI) and therefore suitable for industrial applications.

Table 4-1: Parameters from the isotherm models calculations.

Isotherm model	Differential form	Fitted parameters	Temperature		
			25 °C	35 °C	45 °C
Langmuir	$Q_e = \dfrac{K_L Q_{max} C_e}{1+K_L C_e}$	Q_{max} (mg.g^{-1})	338.93	366.02	420.0
		K_L (L/mg)	0.0864	1.9776	6.5238
		R^2	0.754	0.8681	0.8176
Freundlich	$Q_e = K_F(T)C_e^{1/n_F}$	$K_F\left(L^{\frac{1}{n_F}} mg^{1-\frac{1}{n_F}} g^{-1}\right)$	128.81	181.5	232.2
		n_F	5.61	6.19	6.56
		R^2	0.9769	0.9798	0.9616
Two-surface Langmuir	$Q_e = \dfrac{k_{L,1}(T)Q_{max,1}C_e}{1+k_{L,1}(T)C_e} + \dfrac{k_{L,2}(T)Q_{max,2}C_e}{1+k_{L,2}(T)C_e}$	$K_{L,1}$(L/mg)	0.01145	0.02194	0.0416
		$K_{L,2}$(L/mg)	∞	∞	∞
		Q_1(mg.g^{-1})	262.55	254.41	260.14
		Q_2(mg.g^{-1})	153.89	212.52	259.32
		R^2	0.9966	0.9912	0.9868

4.4 Thermodynamic Properties

Thermodynamic properties of adsorption such as standard enthalpy change ($\Delta H°$), standard entropy change ($\Delta S°$), and standard Gibbs free energy change ($\Delta G°$) were calculated from Equation (2-7). Due to the poor fit of the data to the Langmuir Isotherm (see Table 4-1), the results for the Langmuir isotherm were not used for the thermodynamic analysis. The value of $\Delta S°$, $\Delta H°$ and $\Delta G°$ were calculated from the intercept and the slope of the linear plot of $\ln K$ vs 1/T where the isotherm constants (K_F and K_{L1}) from Freundlich and two-phase Langmuir isotherm models respectively were used to calculate K using Equations (4-1) and (4-2) (Tran, 2016).

$$K = K_L \times M_w \times 55.5 \times 10^3 \tag{4-1}$$

$$K = K_F \times \rho \times \left(\frac{10^6}{\rho}\right)^{1-\frac{1}{n_F}} \qquad (4\text{-}2)$$

With M_W the molecular weight of the adsorbate (116 g/mol), 55.5 mol/L the molar concentration of pure water (mol/L), and ρ the density of pure water (1 g/mL). The various thermodynamic parameters calculated from these models are given in Table 4-2.

The results for the Freundlich and Two-surface Langmuir Isotherm models were significantly similar with positive values of $\Delta S° = 246.8$ and 263.7 J/mol/K was calculated, respectively. This indicates an increase in randomness at the interface of the solution and the catalyst (PANI-NSA/ $Ni Fe_2 O_4$). Additionally, the calculated values of $\Delta H° = 30.3$ and 50.8 kJ/mol, for the Freundlich and Two-surface Langmuir Isotherm models respectively, indicated physical and reversible adsorption processes (Guo *et al*). The positive values of $\Delta H°$ also confirms an endothermic adsorption process. Negative values of $\Delta G°$ were calculated at all the studied temperatures thus proving the spontaneity of the adsorption process. The decrease of $\Delta G°$ with an increase in temperature further shows that the adsorption becomes more favourable at higher temperatures.

Table 4-2: Thermodynamic parameters for adsorption of Cr(VI)

Isotherm	Temperature (K)	$\Delta G°$ (J/mol)	$\Delta H°$ (kJ/mol)	$\Delta S°$ (J/mol/K)	R^2 (linear fit)
Freundlich	298	-43215	30.3	246.8	0.991
	308	-45839			
	318	-48145			
Two-surface Langmuir	298	-27790	50.8	263.7	1.000
	308	-30388			
	318	-33066			

4.5 Adsorption kinetics

The Cr (VI) concentration in the solution as a function of contact time is shown in Figure 4-8 (a). It is observed that the Cr (VI) concentration decreases rapidly in the first 30 minutes followed by a slower decrease until equilibrium is reached. The rapid removal rate observed initially is due to availability of large number of vacant active sites that provide surface for adsorption of Cr (VI). The presence of vacant sites creates adsorption gradient between the adsorbate ions and the adsorbent which leads to the adsorption. As the adsorption progresses, most of the active sites are occupied and thus the decrease in adsorption gradient. When equilibrium is reached, all the active sites are occupied and thus no further change in the removal rate. The time required to reach equilibrium is also observed to depend on initial concentration of Cr (VI) in the solution with more time required for higher initial concentration. Equilibrium is reached within 24 h for all the concentrations studied in this paper and no further change in concentration was observed after 24 h. This is consistent with other results from literature (Muedi *et*

36

al, 2022) which demonstrated an apparent equilibrium after approximately 10 minutes, which was followed by a continued removal of Cr (VI) continuing for as long as 180 minutes. This subsequent slower removal was attributed to a Cr (VI) reduction phase following the initial adsorption. The in-situ reduction of Cr (VI) to Cr (III) after adsorption has been well documented in literature (Chen *et al*, 2018; Liu *et al*, 2021; Liu *et al*, 2023a).
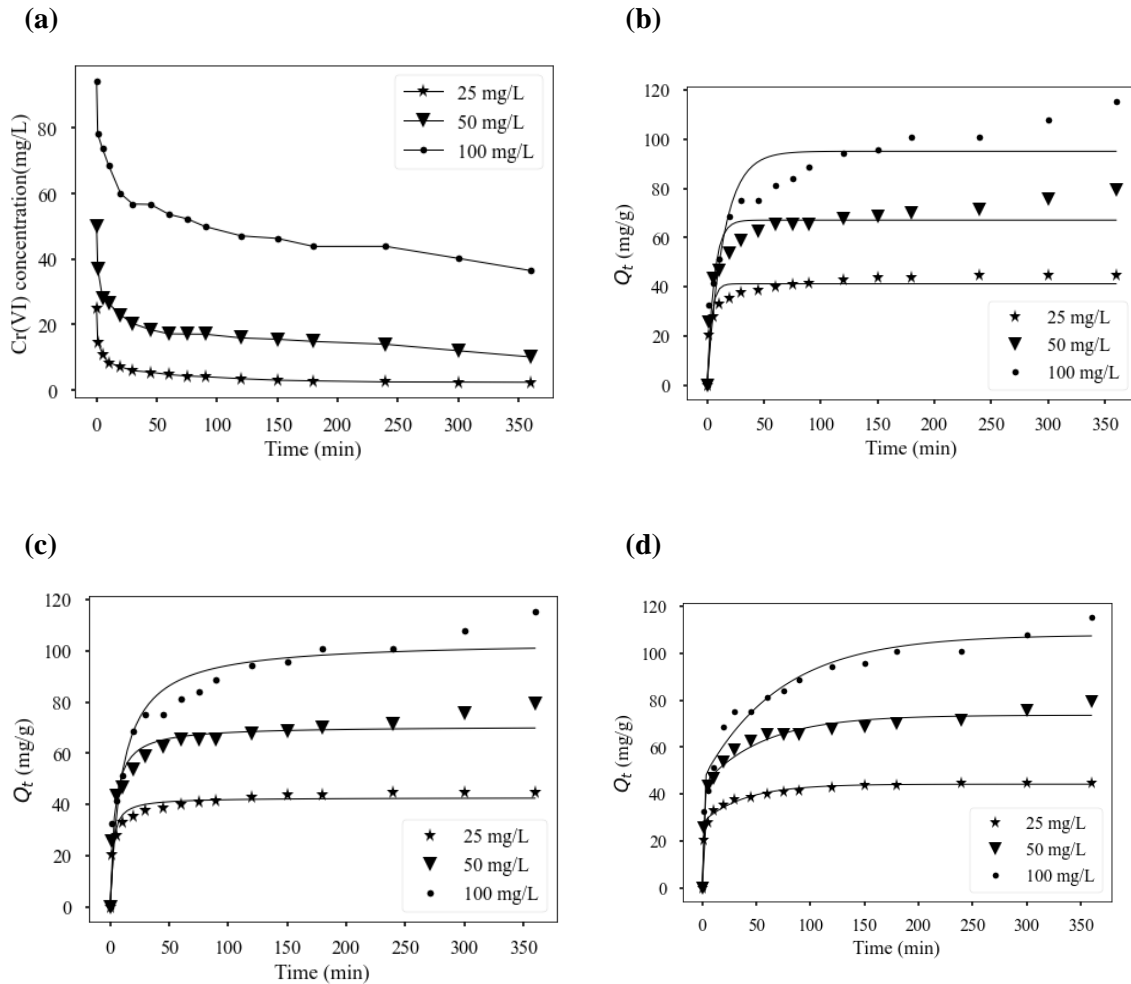
Figure 4-8: The effect of time on concentration (a), (b) pseudo-first order, (c) pseudo-second order and (d) Two-phase adsorption models fitting.

The fitting of the kinetic data on kinetic models is shown in Figure 4-8(b, c, d) and the parameters obtained from the fitting are given in Table 4-3. The two-phase Langmuir model is observed to fit the data more accurately compared to the PFO and PSO models. The rate constant is observed to decrease with an increase in the initial concentration of Cr (VI) for both the PFO and PSO models. The calculated equilibrium uptake of Cr (VI) increases with increase in the initial concentration of Cr (VI) for all models. The rate constants calculated from the TPA model do not follow the trend for the other two models.

37

Table 4-3: Kinetic parameters fitted from the models.

Kinetic model	Differential form	Fitted Parameters	Concentration (mg/L)		
			25	50	100
Pseudo first order	$\dfrac{dQ}{dt} = k_1(Q_e - Q_t) \therefore Q_t = Q_e(1 - e^{-k_1 t})$	Q_e	41.24	67.12	95.10
		k_1	0.2761	0.1672	0.0693
		R^2	0.876	0.875	0.850
Pseudo second order	$\dfrac{dQ_t}{dt} = k_1(Q_e - Q_t)^2 \therefore Q_t = \dfrac{k_2 Q_e^2 t}{1 + k_2 Q_e t}$	k_2	0.0118	0.00384	0.00095
		Q_e	42.7	70.58	103.88
		R^2	0.9523	0.9461	0.9232
Two phase adsorption	$\begin{cases} \dfrac{dQ_{t,fast}}{dt} = k_{fast}(Q_{e,fast} - Q_{t,fast}), \\ \dfrac{dQ_{t,slow}}{dt} = k_{slow}(Q_{e,slow} - Q_{t,slow}) \\ Q_{t,fast} + Q_{t,slow} = Q_t \\ Q_{e,fast} + Q_{e,slow} = Q_e \end{cases}$ $\therefore Q_t = Q_{e,fast}(1 - e^{-k_{fast}t})$ $+ (Q_e - Q_{e,fast})(1 - e^{-k_{slow}t})$	k_{slow}	0.02547	0.01795	0.0139
		k_{fast}	1.272	0.8401	1.1485
		$q_{e,slow}$	16.28	30.2	62.031
		$q_{e,fast}$	27.97	43.41	45.79
		R^2	0.9941	0.985	0.9774

4.6 Effect of competing ions

In industries where chromium is used such as electroplating, paint production, and paper and dye manufacturing, a few other metals are also used and hence the discharge wastewater may contain other metals such as zinc, copper, metal sulfate, and metal nitrates (Bhaumik *et al*, 2018). Figure 4-9 shows the effect of other ions (copper (Cu^{2+}), zinc (Zn^{2+}), sulfate (SO_4^{2-}) and nitrate (NO_3^-)) on the Cr (VI) removal efficiency. An insignificant increase in the percentage removal of Cr (VI) is observed in the presence of other ions even when their concentrations is increased. The percentage removal of Cr (VI) increases from 94 % to 96.8 % when the concentration of other ions is increased from 50 to 150 mg/L. The results suggest that the competing ions have no significant effect on the overall effectiveness of the PANI-NSA/Ni Fe_2O_4 in the removal of Cr (VI). A further study to check effect of individual ions is suggested for a better conclusion.

38
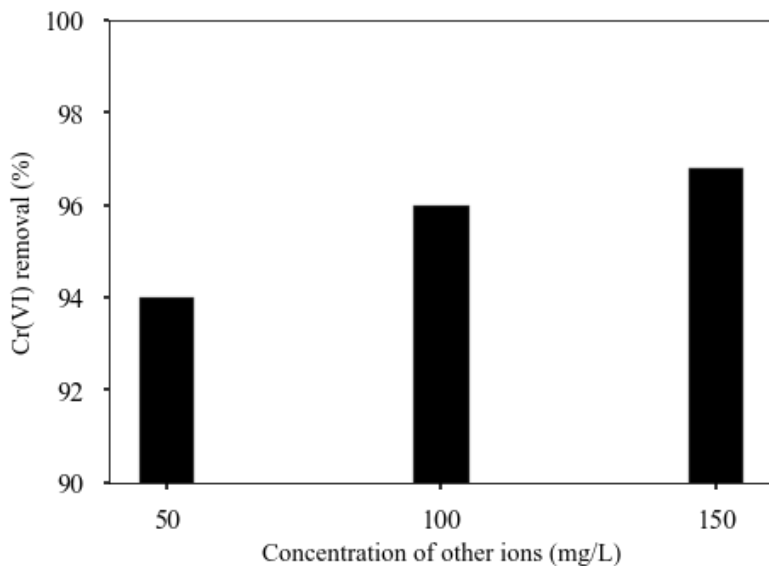
Figure 4-9: Effect other ions on the removal of Cr (VI).

4.7 Reusability studies

Reusability studies were done to determine the ability of PANI-NSA/ Ni Fe$_2$O$_4$ to be re-used in the removal of Cr (VI). The results are shown in Figure 4-10. The material could effectively be recovered and re-used for 5 cycles. A slight decline in Cr (VI) was observed after the second adsorption cycle of using PANI-NSA/ Ni Fe$_2$O$_4$ indicating a change in chemical composition of the material after a second cycle. The Cr (VI) removal efficiency is still above 80% for the first 3 cycles which indicates that PANI-NSA/Ni Fe$_2$O$_4$ is effective and can be reused. These results further confirm that PANI-NSA/Ni Fe$_2$O$_4$ is an excellent adsorbent for industrial application.

Figure 4-10: Recycling of PANI-NSA/ Ni Fe$_2$O$_4$ for the removal of Cr (VI)

39

4.8 Test on real chromium water

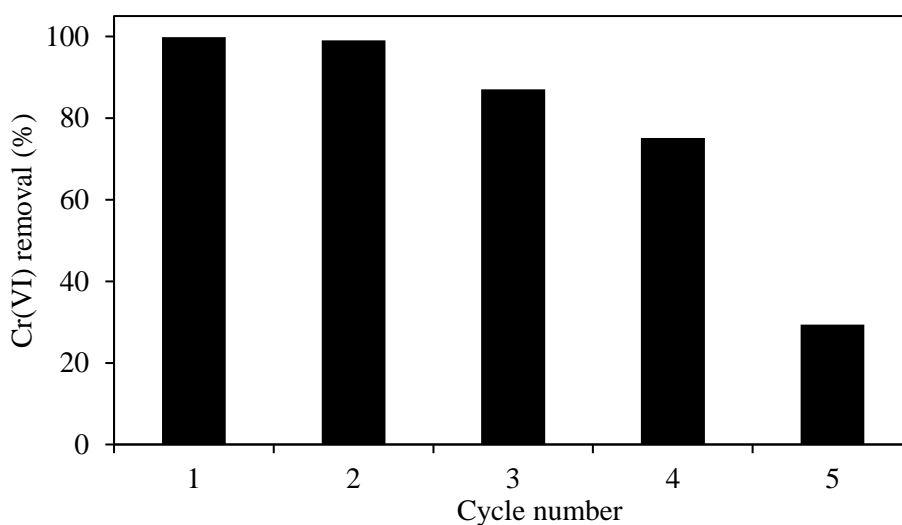An effect of dose study with real chromium wastewater was done and the results are shown in Figure *4-11*. The results show that the removal efficiency of PANI-NSA/Ni Fe_2O_4 is slightly lower when using real chromium wastewater compared to when using the synthetic wastewater. This could be due to the presence of other competing ions in the real wastewater. The removal efficiency is observed to increase with an increase in dosage with a complete removal observed at 40 mg dosage. These results are consistent with effect of dosage study on synthetic water and therefore confirm that PANI-NSA/Ni Fe_2O_4 can be applied in removal of Cr (VI) from industrial wastewater.
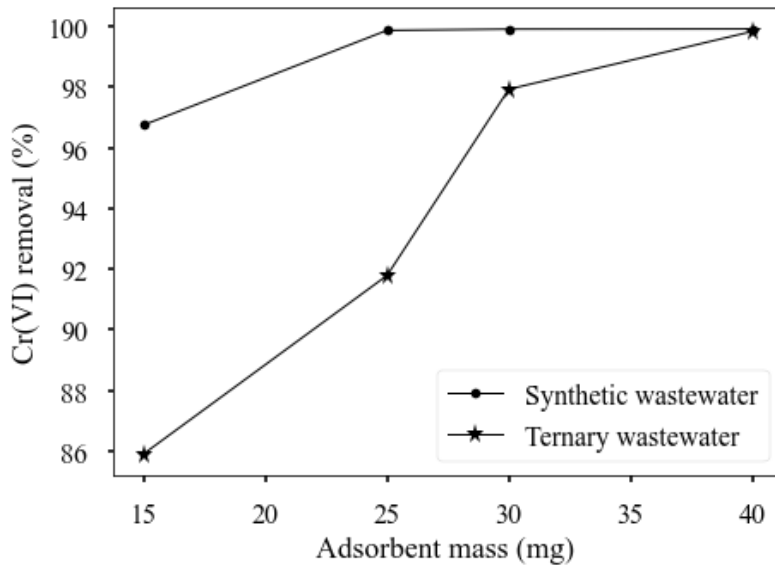
Figure 4-11: Effect of dose study on real chromium water

4.9 Leaching test

Leaching studies confirmed the presence of and Ni and Fe in the solution both after adsorption and desorption procedures at pH 2. This indicates that the synthesized PANI-NSA/Ni Fe_2O_4 is not very stable in acidic conditions. Further studies to check the stability of PANI-NSA/Ni Fe_2O_4 in other pH conditions is recommended.

4.10 Comparison with other adsorbents

A comparison of maximum adsorption capacity between PANI-NSA/Ni Fe_2O_4 and other adsorbents was done and is given in Table 4-4.

Table 4-4: Comparison of PANI-NSA/Ni Fe_2O_4 and other PANI based adsorbents studied for Cr (VI) removal.

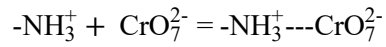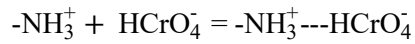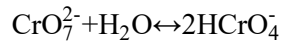| Name of the material	Q_m (mg/g)	Temperature (°C)	pH	Reference
Polypyrrole/Fe_3O_4 nanocomposite	169.49	25	2.0	Bhaumik *et al* (2013)
Polypyrrole/maghemite	209	Room temperature	2.0	Chávez-Guajardo *et al* (2015)
Polyaniline/maghemite	196	Room temperature	2.0	Chávez-Guajardo *et al* (2015)
Polyaniline-coated date seed biochar	27.3	50	5.0	Tripathy *et al* (2021)
Polyaniline@ magnetic chitosan	186.6	25	2.0	Lei *et al* (2020)
Polyaniline/ZnO	120.92	30	2.0	Ahmad (2019)
Polyaniline	198.67	15	3.0	Zhu *et al* (2016)
Polyaniline coated PVDF-HFP	15.08	24	4.5	Dognani *et al* (2019)
Tea waste/Fe_3O_4	75.76	45	2	Fan *et al* (2017)
PANI-NSA/ Ni Fe_2O_4	420.0	45	2.0	This study

4.11 Proposed mechanism of adsorption

Figure 4-12 (a) shows the comparison between the total Cr and Cr (VI) available in the solution after adsorption. The comparison between total chromium and Cr (VI) concentration with time (Figure 4-12 (b)) shows that initially total Cr is equal to Cr (VI) thus no Cr (III) present. As the time goes, the total chromium is more than Cr (VI) thus presence of Cr (III). The presence of Cr (III) in the solution proves that some of the Cr (VI) gets adsorbed by PANI-NSA/ Ni Fe_2O_4 is reduced to Cr (III) which is released back to the solution. The deconvoluted chromium peaks from the XPS (Figure 4-12 (c)) shows the presence of both Cr (VI) and Cr (III) on the surface of PANI-NSA/ Ni Fe_2O_4 which further confirms the reduction of Cr (VI) to Cr (III).

Therefore, from the XPS results and the comparison between total chromium and Cr (VI) present in the solution, the mechanism of Cr (VI) removal by PANI-NSA/ Ni Fe_2O_4 involves adsorption of Cr (VI) onto the surface of PANI-NSA/Ni Fe_2O_4 and then reduction of Cr (VI) to Cr (III). Some of the Cr (III) is adsorbed onto the PANI-NSA/Ni Fe_2O_4 surface while part of the Cr (III) is released back into the solution. Consequently, Cr (VI) removal is believed to occur in two stages:

1. In acidic conditions (in the pH range 2 to 6), dichromate oxyanion is hydrolysed to $HCrO_4^-$ which electrostatically interacts with the positively charged amine groups from PANI-NSA/Ni Fe_2O_4 while at higher pH values (above 6), dichromate oxyanions are the most valent and are removed by binding with the protonated amine group from PANI-NSA/Ni Fe_2O_4 leading to Cr (VI) removal via adsorption:

$$CrO_7^{2-}+H_2O \leftrightarrow 2HCrO_4^-$$

$$-NH_3^+ + HCrO_4^- = -NH_3^+ ---HCrO_4^-$$

$$-NH_3^+ + CrO_7^{2-} = -NH_3^+ ---CrO_7^{2-}$$

2. Cr (VI) is subsequently reduced to Cr (III) due to presence of electron donors of PANI:

$$HCrO_4^- + 7H^+ + 3e^- \leftrightarrow Cr^{3+} + 4H_2O$$
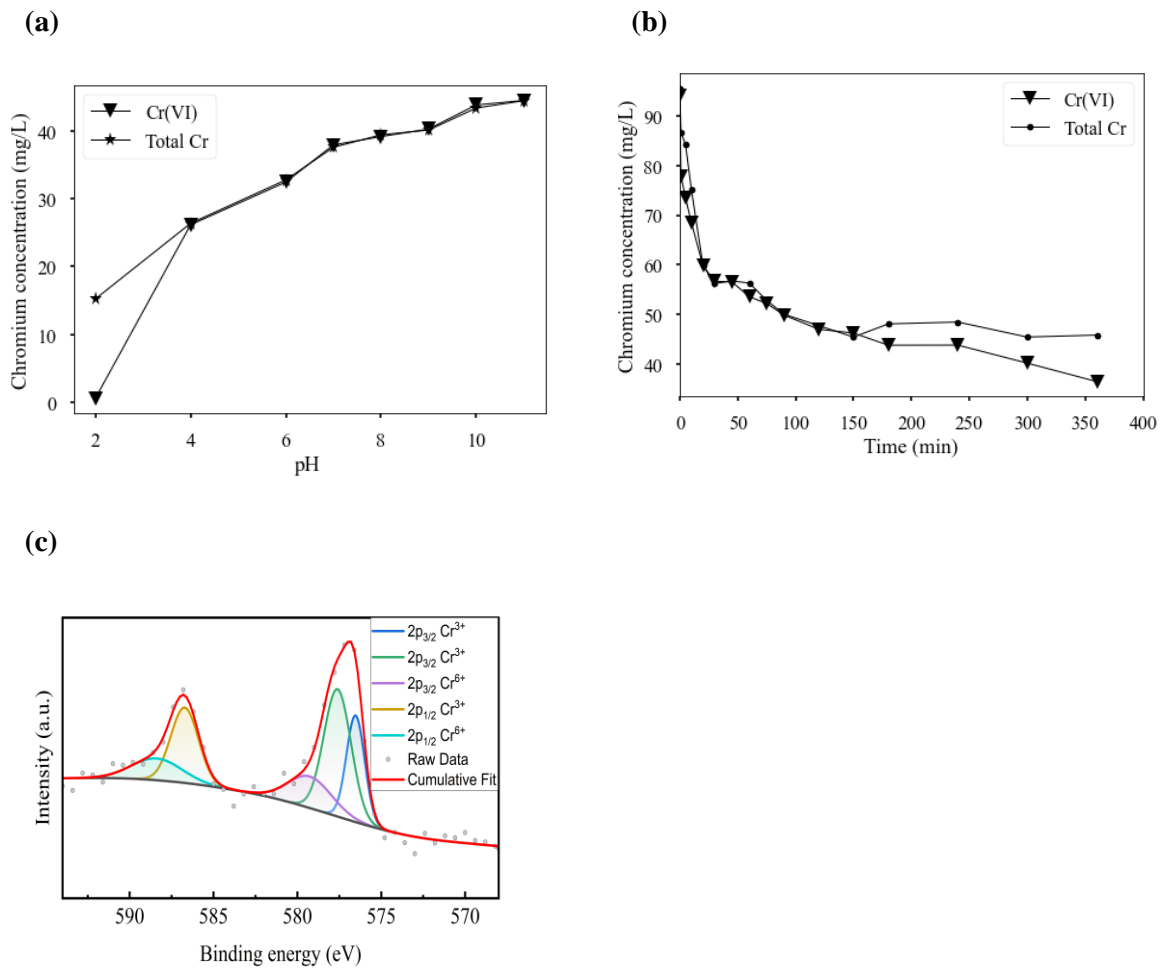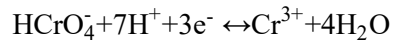
(a)

(b)

(c)

Figure 4-12: Concentration of Cr (VI) and total chromium under different parameters (a) pH and (b) contact time and (c) XPS speciation analysis of chromium.
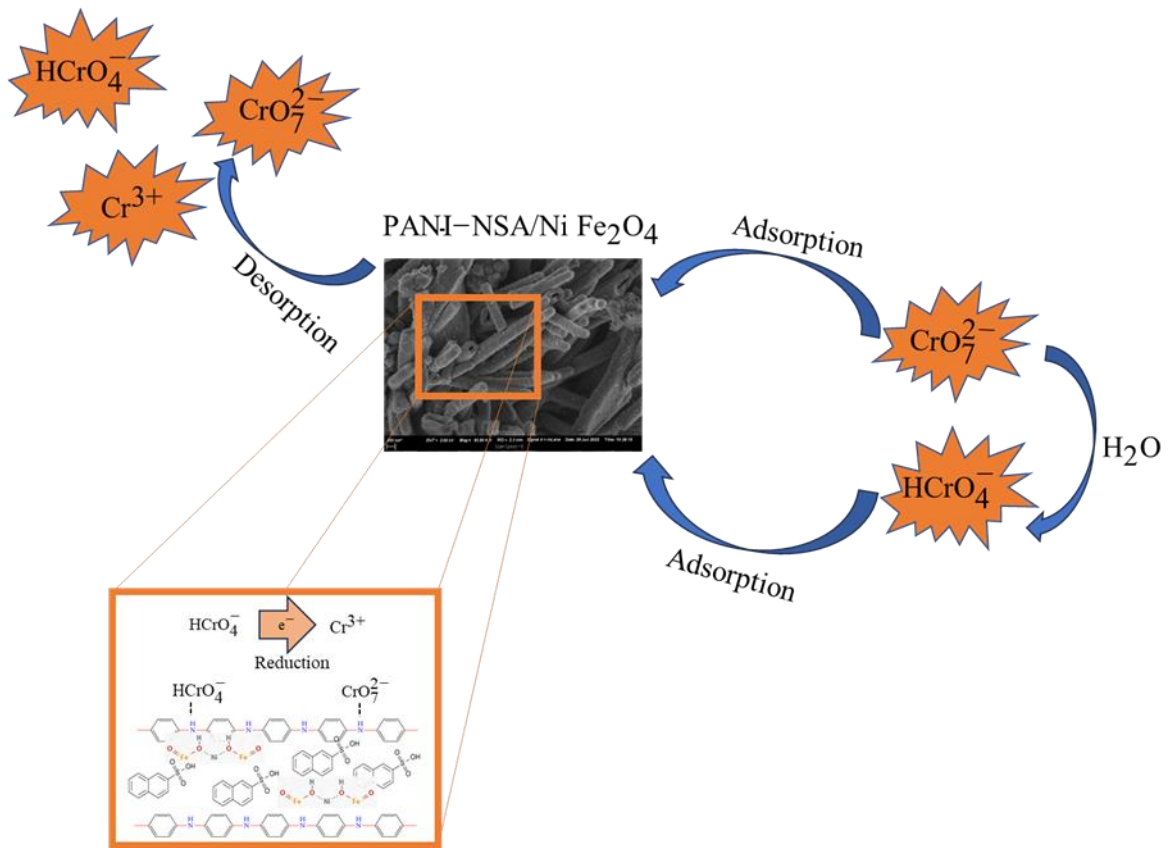
Figure 4-13: proposed mechanism of Cr (VI) removal by PANI-NSA/Ni Fe$_2$O$_4$

Chapter 5   Conclusion and Recommendations

The removal of Cr (VI) from aqueous solution using PANI-NSA/NiFe$_2$O$_4$ nanocomposite was studied. Based on the objectives of the study the following conclusions were made:

1. Characterization studies showed that the nanoparticles attach onto the surface of the forming polymer which is tubular in shape. Surface functional groups determined by XPS proved that Cr (VI) is reduced to Cr (III) which attaches on the surface of PANI-NSA/NiFe$_2$O$_4$ with some released back into the solution.

2. The maximum removal efficiency (99%) of Cr (VI) was observed at a pH value of 2 and adsorbent loading of 0.5 g/L. The removal efficiency also increased with an increase in temperature and contact time at constant concentration.

3. A maximum adsorption capacity of 420 mg/g at 45°C was calculated using the Langmuir isotherm model. Compared to other materials from the literature, the adsorption capacity of PANI-NSA/NiFe$_2$O$_4$ was higher. The two-phase Langmuir kinetic model best fitted the kinetic data from the experiment.

4. The effect of other ions on the removal of Cr (VI) was minimal proving that the material is effective even in the presence of other ions and hence can effectively be applied in industrial wastewater treatment.

5. Up to 87% Cr (VI) removal efficiency could be achieved for three adsorption cycles, hence PANI-NSA/NiFe$_2$O$_4$ can effectively be recycled. When using real chromium wastewater, it was observed that 40 mg of PANI-NSA/NiFe$_2$O$_4$ could achieve 100 % Cr (VI) removal efficiency from 50 mL solution with 50 mg/L initial concentration.

Based on these conclusions, the following recommendations can be considered for future studies:

1. Further investigation on the specific mechanisms underlying the reduction of Cr (VI) to Cr (III) on the surface of the nanocomposite in greater detail. The use of advanced techniques such in-situ spectroscopy or computational modelling is recommended.

2. Investigate the long term-term stability and performance of PANI-NSA/NiFe$_2$O$_4$ nanocomposite in a continuous flow systems or real-world wastewater treatment scenarios.

3. Develop and test efficient regeneration techniques for PANI-NSA/NiFe$_2$O$_4$ nanocomposite to maximize its reusability.

4. Conduct an assessment of the environmental impact of using PANI-NSA/NiFe$_2$O$_4$ nanocomposite in wastewater treatment.

5. Conduct in-depth investigations into the mechanisms of how different ions present in industrial wastewater affect the removal efficiency of Cr (VI) using the nanocomposite to understand the selectivity of the material.

6. Investigate ways to enhance the sustainability of the synthesis process and consider incorporating green chemistry principles into the production of PANI-NSA/NiFe$_2$O$_4$ nanocomposite.

7. Explore the scalability of the synthesis process for PANI-NSA/NiFe$_2$O$_4$ nanocomposite to meet the demands of industrial wastewater treatment by exploring the cost effectiveness of large scale production and application.

References

Abdel-Halim, ES, and Al-Deyab, SS (2011), "Removal of heavy metals from their aqueous solutions through adsorption onto natural polymers" *Carbohydrate Polymers*, 84(1), 454-458.

Abushawish, A, Almanassra, IW, Backer, SN, Jaber, L, Khalil, AK, Abdelkareem, MA, Sayed, ET, Alawadhi, H, Shanableh, A, and Atieh, MA (2022), "High-efficiency removal of hexavalent chromium from contaminated water using nitrogen-doped activated carbon: Kinetics and isotherm study" *Materials Chemistry and Physics*, 291126758.

Affairs, TDoE (2012), Highveld Priority Area Air Quality Management Plan. *In:* Africa, EARoS (ed.).

Agarwal, M, and Singh, K (2017), "Heavy metal removal from wastewater using various adsorbents: a review" *Journal of Water Reuse and Desalination*, 7(4), 387-419.

Agrawal, S, and Singh, N (2016), "Removal of toxic hexavalent chromium from aqueous solution by nickel ferrite-polyaniline nanocomposite" *Desalination and Water Treatment*, 57(38), 17757-17766.

Ahmad, R (2019), "Polyaniline/ZnO nanocomposite: a novel adsorbent for the removal of Cr (VI) from aqueous solution" *Advances in composite materials development*, 1-22.

Aigbe, UO, Das, R, Ho, WH, Srinivasu, V, and Maity, A (2018), "A novel method for removal of Cr (VI) using polypyrrole magnetic nanocomposite in the presence of unsteady magnetic fields" *Separation and Purification Technology*, 194377-387.

Al-Dhabi, NA, Esmail, GA, and Valan Arasu, M (2020), "Sustainable conversion of palm juice wastewater into extracellular polysaccharides for absorption of heavy metals from Saudi Arabian wastewater" *Journal of Cleaner Production*, 277124252.

Alamier, WM, Hasan, N, Nawaz, MS, Ismail, KS, Shkir, M, Malik, MA, and Oteef, MD (2023), "Biosynthesis of NiFe2O4 nanoparticles using Murayya koenigii for photocatalytic dye degradation and antibacterial application" *Journal of Materials Research and Technology*, 221331-1348.

Amin, KF, Gulshan, F, Asrafuzzaman, FNU, Das, H, Rashid, R, and Manjura Hoque, S (2023), "Synthesis of mesoporous silica and chitosan-coated magnetite nanoparticles for heavy metal adsorption from wastewater" *Environmental Nanotechnology, Monitoring & Management*, 20100801.

Anjum, A, Mazari, SA, Hashmi, Z, Jatoi, AS, Abro, R, Bhutto, AW, Mubarak, NM, Dehghani, MH, Karri, RR, and Mahvi, AH (2023), "A review of novel green adsorbents as a sustainable alternative for the remediation of chromium (VI) from water environments" *Heliyon*.

Ao, W, Fu, J, Mao, X, Kang, Q, Ran, C, Liu, Y, Zhang, H, Gao, Z, Li, J, and Liu, G (2018), "Microwave assisted preparation of activated carbon from biomass: A review" *Renewable and Sustainable Energy Reviews*, 92958-979.

Arbabi, M, Hemati, S, and Amiri, M (2015), "Removal of lead ions from industrial wastewater: A review of Removal methods" *International Journal of Epidemiologic Research*, 2(2), 105-109.

Arslan, H, Eskikaya, O, Bilici, Z, Dizge, N, and Balakrishnan, D (2022), "Comparison of Cr (VI) adsorption and photocatalytic reduction efficiency using leonardite powder" *Chemosphere*, 300134492.

Asanu, M, Beyene, D, and Befekadu, A (2022), "Removal of Hexavalent Chromium from Aqueous Solutions Using Natural Zeolite Coated with Magnetic Nanoparticles: Optimization, Kinetics, and Equilibrium Studies" *Adsorption Science & Technology*, 2022.

Ayawei, N, Ebelegi, AN, and Wankasi, D (2017), "Modelling and interpretation of adsorption isotherms" *Journal of chemistry*, 2017.

Azimi, A, Azari, A, Rezakazemi, M, and Ansarpour, M (2017), "Removal of heavy metals from industrial wastewaters: a review" *ChemBioEng Reviews*, 4(1), 37-59.

Bakar, SA, Mohamed, RMSR, Al-Gheethi, A, Khamidun, MH, Musa, S, and Soon, CF (2023), "Kinetics and isotherms of heavy metals removal from laundry greywater by chitosan ceramic beads" *Environmental Advances*, 13100391.

Bampaiti, A, Noli, F, and Misaelides, P (2013), "Investigation of the Cr (VI) removal from aqueous solutions by stabilized iron-nanoparticles using 51 Cr-tracer" *Journal of Radioanalytical and Nuclear Chemistry*, 298909-914.

Bánfalvi, G (2011), Cellular effects of heavy metals, Springer,

Basavaraja, C, Il Kim, K, Ho Jung, G, and Sung Huh, D (2014), "Electrical properties of colloidal polyaniline-2-naphthalene sulfonic acid/graphene nanoparticle composite films" *Polymer Composites*, 35(1), 60-67.

Beygisangchin, M, Abdul Rashid, S, Shafie, S, Sadrolhosseini, AR, and Lim, HN (2021), "Preparations, properties, and applications of polyaniline and polyaniline thin films—A review" *Polymers*, 13(12), 2003.

Bhadra, S, Singha, NK, and Khastgir, D (2007), "Electrochemical synthesis of polyaniline and its comparison with chemically synthesized polyaniline" *Journal of applied polymer science*, 104(3), 1900-1904.

Bhaumik, M, Gupta, VK, and Maity, A (2018), "Synergetic enhancement of Cr (VI) removal from aqueous solutions using polyaniline@ Ni (OH) 2 nanocomposites adsorbent" *Journal of environmental chemical engineering*, 6(2), 2514-2527.

Bhaumik, M, Maity, A, and Brink, HG (2021), "Zero valent nickel nanoparticles decorated polyaniline nanotubes for the efficient removal of Pb (II) from aqueous solution: Synthesis, characterization and mechanism investigation" *Chemical Engineering Journal*, 417127910.

Bhaumik, M, Maity, A, Mahule, T, and Srinivasu, V (2019), "Tunability of localization length in naphthalene sulfonic acid doped polyaniline/nickel ferrite composite nanorods system" *Journal of Applied Physics*, 126(3), 035102.

Bhaumik, M, Setshedi, K, Maity, A, and Onyango, MS (2013), "Chromium (VI) removal from water using fixed bed column of polypyrrole/Fe3O4 nanocomposite" *Separation and Purification Technology*, 11011-19.

Bibi, S, Ahmad, A, Anjum, MAR, Haleem, A, Siddiq, M, Shah, SS, and Al Kahtani, A (2021), "Photocatalytic degradation of malachite green and methylene blue over reduced graphene oxide (rGO) based metal oxides (rGO-Fe3O4/TiO2) nanocomposite under UV-visible light irradiation" *Journal of environmental chemical engineering*, 9(4), 105580.

Birniwa, AH, Kehili, S, Ali, M, Musa, H, Ali, U, Kutty, SRM, Jagaba, AH, Abdullahi, SSa, Tag-Eldin, EM, and Mahmud, HNME (2022), "Polymer-based nano-adsorbent for the removal of lead ions: kinetics studies and optimization by response surface methodology" *Separations*, 9(11), 356.

Bora, AJ, and Dutta, RK (2019), "Removal of metals (Pb, Cd, Cu, Cr, Ni, and Co) from drinking water by oxidation-coagulation-absorption at optimized pH" *Journal of Water Process Engineering*, 31100839.

Carolin, CF, Kumar, PS, Saravanan, A, Joshiba, GJ, and Naushad, M (2017), "Efficient techniques for the removal of toxic heavy metals from aquatic environment: A review" *Journal of environmental chemical engineering*, 5(3), 2782-2799.

Castellar-Ortega, G, Mendoza, E, Angulo, E, Paula, Z, Rosso, M, and Jaramillo, J (2019), "Equilibrium, kinetic and thermodynamic of direct blue 86 dye adsorption on activated carbon obtained from manioc husk" *Revista MVZ Córdoba*, 24(2), 7231-7238.

Chatterjee, S, Sarkar, S, and Bhattacharya, S (2014), "Toxic metals and autophagy" *Chemical research in toxicology*, 27(11), 1887-1900.

Chávez-Guajardo, AE, Medina-Llamas, JC, Maqueira, L, Andrade, CA, Alves, KG, and de Melo, CP (2015), "Efficient removal of Cr (VI) and Cu (II) ions from aqueous media by use of

polypyrrole/maghemite and polyaniline/maghemite magnetic nanocomposites" *Chemical Engineering Journal*, 281826-836.

Chen, C, Liu, Q, Chen, W, Li, F, Xiao, G, Chen, C, Li, R, and Zhou, J (2022), "A high absorbent PVDF composite membrane based on β-cyclodextrin and ZIF-8 for rapid removing of heavy metal ions" *Separation and Purification Technology*, 292120993.

Chen, Y, An, D, Sun, S, Gao, J, and Qian, L (2018), "Reduction and removal of chromium VI in water by powdered activated carbon" *Materials*, 11(2), 269.

Coetzee, JJ, Bansal, N, and Chirwa, EM (2020), "Chromium in environment, its toxic effect from chromite-mining and ferrochrome industries, and its possible bioremediation" *Exposure and health*, 12(1), 51-62.

Cornelissen, G, van Noort, PCM, Parsons, JR, and Govers, HAJ (1997), "Temperature Dependence of Slow Adsorption and Desorption Kinetics of Organic Compounds in Sediments" *Environmental Science & Technology*, 31(2), 454-460.

Dąbrowski, A, Hubicki, Z, Podkościelny, P, and Robens, E (2004), "Selective removal of the heavy metal ions from waters and industrial wastewaters by ion-exchange method" *Chemosphere*, 56(2), 91-106.

Das, R, Sypu, VS, Paumo, HK, Bhaumik, M, Maharaj, V, and Maity, A (2019), "Silver decorated magnetic nanocomposite (Fe3O4@ PPy-MAA/Ag) as highly active catalyst towards reduction of 4-nitrophenol and toxic organic dyes" *Applied Catalysis B: Environmental*, 244546-558.

de Saussure, T (1812), Observations sur l'absorption des gaz par différens corps,

Demirbas, E, Kobya, M, Senturk, E, and Ozkan, T (2004), "Adsorption kinetics for the removal of chromium (VI) from aqueous solutions on the activated carbons prepared from agricultural wastes" *Water Sa*, 30(4), 533-539.

Dognani, G, Hadi, P, Ma, H, Cabrera, FC, Job, AE, Agostini, DL, and Hsiao, BS (2019), "Effective chromium removal from water by polyaniline-coated electrospun adsorbent membrane" *Chemical Engineering Journal*, 372341-351.

Driscoll, T, Barber, J, Chandran, K, Constable, S, Darnell, C, DiMenna, R, Gaines, B, Goodman, A, Hlavek, R, and Johns, F (2008), "Industrial wastewater management, treatment and disposal" *WEF Manual of Practice No. FD-3rd; Mcgraw-Hill: New York, NY, USA*, 474-489.

Durai, G, and Rajasimman, M (2011), "Biological treatment of tannery wastewater-a review" *Journal of Environmental science and Technology*, 4(1), 1-17.

El-Kafrawy, AF, El-Saeed, SM, Farag, RK, El-Saied, HA-A, and Abdel-Raouf, ME-S (2017), "Adsorbents based on natural polymers for removal of some heavy metals from aqueous solution" *Egyptian Journal of Petroleum*, 26(1), 23-32.

Fan, S, Wang, Y, Li, Y, Tang, J, Wang, Z, Tang, J, Li, X, and Hu, K (2017), "Facile synthesis of tea waste/Fe 3 O 4 nanoparticle composite for hexavalent chromium removal from aqueous solution" *RSC advances*, 7(13), 7576-7590.

Farhan, A, Zulfiqar, M, Rashid, EU, Nawaz, S, Iqbal, HM, Jesionowski, T, Bilal, M, and Zdarta, J (2023), "Removal of Toxic Metals from Water by Nanocomposites through Advanced Remediation Processes and Photocatalytic Oxidation" *Current Pollution Reports*, 1-21.

Feng, J, Xiong, S, Ren, L, and Wang, Y (2022), "Atomic layer deposition of TiO2 on carbon-nanotubes membrane for capacitive deionization removal of chromium from water" *Chinese Journal of Chemical Engineering*, 4515-21.

Fontana, F (1777), "Encyclopedia of surface and colloid science" *Memorie Mat. Soc. Ital. Sci*, 679.

Freundlich, H (1907), "Über die Adsorption in Lösungen" *Zeitschrift für Physikalische Chemie*, 57U(1), 385-470.

Fungene, T, Ndlovu, S, and Matinde, E (2023), "Scale formation in wet scrubbers and the current state of anti-scaling and softening methods for hard waters: A review" *Separation Science and Technology*, 58(7), 1331-1346.

Garg, S, Singhal, S, and Goel, N (2022), "Experimental and computational investigation on Polyaniline/Zno nanocomposite for dye adsorption" *Materials Science and Engineering: B*, 284115895.

Gautam, A, Kushwaha, A, and Rani, R (2021), Microbial remediation of hexavalent chromium: An eco-friendly strategy for the remediation of chromium-contaminated wastewater. *The future of effluent treatment plants.* Elsevier.

Geng, J, Lin, L, Gu, F, and Chang, J (2022), "Adsorption of Cr (VI) and dyes by plant leaves: Effect of extraction by ethanol, relationship with element contents and adsorption mechanism" *Industrial Crops and Products*, 177114522.

George William, K, Serkan, E, Atakan, Ö, Özcan, HK, and Serdar, A (2018), Modelling of Adsorption Kinetic Processes—Errors, Theory and Application. *In:* Serpil, E (ed.) *Advanced sorption process applications.* Rijeka: IntechOpen.

Ghangrekar, M, and Chatterjee, P (2018), "Water pollutants classification and its effects on environment" *Carbon nanotubes for clean water*, 11-26.

Giri, AK (2012) "Removal of arsenic (III) and chromium (VI) from the water using phytoremediation and bioremediation techniques",

Gu, W, and Yushin, G (2014), "Review of nanostructured carbon materials for electrochemical capacitor applications: advantages and limitations of activated carbon, carbide-derived carbon, zeolite-templated carbon, carbon aerogels, carbon nanotubes, onion-like carbon, and graphene" *Wiley Interdisciplinary Reviews: Energy and Environment*, 3(5), 424-473.

Guo, L, Verma, C, and Zhang, D 17.4.1 Physisorption. *Eco-Friendly Corrosion Inhibitors - Principles, Designing and Applications.* Elsevier.

Guo, Z, Cheng, M, Ren, W, Wang, Z, and Zhang, M (2022), "Treated activated carbon as a metal-free catalyst for effectively catalytic reduction of toxic hexavalent chromium" *Journal of Hazardous Materials*, 430128416.

Gupta, K, Joshi, P, Gusain, R, and Khatri, OP (2021), "Recent advances in adsorptive removal of heavy metal and metalloid ions by metal oxide-based nanomaterials" *Coordination Chemistry Reviews*, 445214100.

Gupta, N, Jain, P, Rana, R, and Shrivastava, S (2017), "Current development in synthesis and characterization of nickel ferrite nanoparticle" *Materials Today: Proceedings*, 4(2), 342-349.

Hamadeen, HM, Elkhatib, EA, and Moharem, ML (2022), "Optimization and mechanisms of rapid adsorptive removal of chromium (VI) from wastewater using industrial waste derived nanoparticles" *Scientific Reports*, 12(1), 14174.

Han, S, Zang, Y, Gao, Y, Yue, Q, Zhang, P, Kong, W, Jin, B, Xu, X, and Gao, B (2020), "Co-monomer polymer anion exchange resin for removing Cr (VI) contaminants: Adsorption kinetics, mechanism and performance" *Science of the Total Environment*, 709136002.

Harijan, DK, and Chandra, V (2016), "Polyaniline functionalized graphene sheets for treatment of toxic hexavalent chromium" *Journal of environmental chemical engineering*, 4(3), 3006-3012.

Haseena, M, Malik, MF, Javed, A, Arshad, S, Asif, N, Zulfiqar, S, and Hanif, J (2017), "Water pollution and human health" *Environmental Risk Assessment and Remediation*, 1(3).

Ho, YS, and McKay, G (1999), "Pseudo-second order model for sorption processes" *Process Biochemistry*, 34(5), 451-465.

Hou, L, Yang, C, Rao, X, Hu, L, Bao, Y, Gao, Y, and Zhu, X (2021), "Fabrication of recoverable magnetic surface ion-imprinted polymer based on graphene oxide for fast and selective removal of lead ions from aqueous solution" *Colloids and Surfaces A: Physicochemical and Engineering Aspects*, 625126949.

Hsini, A, Benafqir, M, Naciri, Y, Laabd, M, Bouziani, A, Ez-zahery, M, Lakhmiri, R, El Alem, N, and Albourine, A (2021), "Synthesis of an arginine-functionalized polyaniline@ FeOOH composite with high removal performance of hexavalent chromium ions from water: adsorption behavior, regeneration and process capability studies" *Colloids and Surfaces A: Physicochemical and Engineering Aspects*, 617126274.

Hu, H, and Xu, K (2020), Chapter 8 - Physicochemical technologies for HRPs and risk control. *In:* Ren, H, and Zhang, X (eds.) *High-Risk Pollutants in Wastewater.* Elsevier.

Hu, Q, Lan, R, He, L, Liu, H, and Pei, X (2023), "A critical review of adsorption isotherm models for aqueous contaminants: Curve characteristics, site energy distribution and common controversies" *Journal of Environmental Management*, 329117104.

Hu, S, Liu, C, Bu, H, Chen, M, and Fei, Y-h (2024), "Efficient reduction and adsorption of Cr(VI) using FeCl3-modified biochar: Synergistic roles of persistent free radicals and Fe(II)" *Journal of Environmental Sciences*, 137626-638.

Ibrahim, BM, and Fakhre, NA (2019), "Crown ether modification of starch for adsorption of heavy metals from synthetic wastewater" *International Journal of Biological Macromolecules*, 12370-80.

Isiuku, BO, Okonkwo, PC, and Emeagwara, CD (2021), "Batch adsorption isotherm models applied in single and multicomponent adsorption systems–a review" *Journal of Dispersion Science and Technology*, 42(12), 1879-1897.

Jahan, K, Kumar, N, and Verma, V (2018), "Removal of hexavalent chromium from potable drinking using a polyaniline-coated bacterial cellulose mat" *Environmental Science: Water Research & Technology*, 4(10), 1589-1603.

Javadian, H, Vahedian, P, and Toosi, M (2013), "Adsorption characteristics of Ni (II) from aqueous solution and industrial wastewater onto Polyaniline/HMS nanocomposite powder" *Applied Surface Science*, 28413-22.

Jaymand, M (2013), "Recent progress in chemical modification of polyaniline" *Progress in Polymer Science*, 38(9), 1287-1306.

Jiang, Y, Liu, Z, Zeng, G, Liu, Y, Shao, B, Li, Z, Liu, Y, Zhang, W, and He, Q (2018), "Polyaniline-based adsorbents for removal of hexavalent chromium from aqueous solution: a mini review" *Environmental Science and Pollution Research*, 25(7), 6158-6174.

Kajjumba, GW, Emik, S, Öngen, A, Özcan, HK, and Aydın, S (2018), "Modelling of adsorption kinetic processes—errors, theory and application" *Advanced sorption process applications*, 1-19.

Karić, N, Vukčević, M, Maletić, M, Dimitrijević, S, Ristić, M, Grujić, AP, and Trivunac, K (2023), "Physico-chemical, structural, and adsorption properties of amino-modified starch derivatives for the removal of (in)organic pollutants from aqueous solutions" *International Journal of Biological Macromolecules*, 241124527.

Karimi-Maleh, H, Ayati, A, Ghanbari, S, Orooji, Y, Tanhaei, B, Karimi, F, Alizadeh, M, Rouhi, J, Fu, L, and Sillanpää, M (2021), "Recent advances in removal techniques of Cr (VI) toxic ion from aqueous solution: a comprehensive review" *Journal of Molecular Liquids*, 329115062.

Karthik, R, and Meenakshi, S (2014), "Removal of hexavalent chromium ions using polyaniline/silica gel composite" *Journal of Water Process Engineering*, 137-45.

Keng, P-S, Lee, S-L, Ha, S-T, Hung, Y-T, and Ong, S-T (2014), "Removal of hazardous heavy metals from aqueous environment by low-cost adsorption materials" *Environmental Chemistry Letters*, 1215-25.

Kera, NH, Bhaumik, M, Pillay, K, Ray, SS, and Maity, A (2017), "Selective removal of toxic Cr (VI) from aqueous solution by adsorption combined with reduction at a magnetic nanocomposite surface" *Journal of Colloid and Interface Science*, 503214-228.

Khan, KM, Chakraborty, R, Bundschuh, J, Bhattacharya, P, and Parvez, F (2020), "Health effects of arsenic exposure in Latin America: An overview of the past eight years of research" *Science of the Total Environment*, 710136071.

Kharazi, P, Rahimi, R, and Rabbani, M (2019), "Copper ferrite-polyaniline nanocomposite: structural, thermal, magnetic and dye adsorption properties" *Solid State Sciences*, 9395-100.

Khurshid, H, Mustafa, MRU, and Isa, MH (2022), "Adsorption of chromium, copper, lead and mercury ions from aqueous solution using bio and nano adsorbents: A review of recent trends in the application of AC, BC, nZVI and MXene" *Environmental Research*, 212113138.

Kumar, N, and Joshi, NC (2022), "Adsorption applications of synthetically prepared PANI-CuO based nanocomposite material" *Journal of the Indian Chemical Society*, 99(7), 100551.

Kumar, R, Barakat, M, Taleb, MA, and Seliem, MK (2020), "A recyclable multifunctional graphene oxide/SiO2@ polyaniline microspheres composite for Cu (II) and Cr (VI) decontamination from wastewater" *Journal of Cleaner Production*, 268122290.

Lagergren, SK (1898), "About the theory of so-called adsorption of soluble substances" *Sven. Vetenskapsakad. Handingarl*, 241-39.

Lala, MA, Ntamu, TE, Adesina, OA, Popoola, LT, Yusuff, AS, and Adeyi, AA (2023), "Adsorption of hexavalent chromium from aqueous solution using cationic modified rice husk: Parametric optimization via Taguchi design approach" *Scientific African*, 20e01633.

Langmuir, I (1918), "The adsorption of gases on plane surfaces of glass, mica and platinum" *Journal of the American Chemical Society*, 40(9), 1361--1403.

Larraza, I, López-Gónzález, M, Corrales, T, and Marcelo, G (2012), "Hybrid materials: magnetite–polyethylenimine–montmorillonite, as magnetic adsorbents for Cr (VI) water treatment" *Journal of Colloid and Interface Science*, 385(1), 24-33.

Lei, C, Wang, C, Chen, W, He, M, and Huang, B (2020), "Polyaniline@ magnetic chitosan nanomaterials for highly efficient simultaneous adsorption and in-situ chemical reduction of hexavalent chromium: Removal efficacy and mechanisms" *Science of the Total Environment*, 733139316.

Lingamdinne, LP, Koduru, JR, Choi, Y-L, Chang, Y-Y, and Yang, J-K (2016), "Studies on removal of Pb (II) and Cr (III) using graphene oxide based inverse spinel nickel ferrite nano-composite as sorbent" *Hydrometallurgy*, 16564-72.

Lingegowda, DC, Kumar, JK, Prasad, AD, Zarei, M, and Gopal, S (2012), "FTIR spectroscopic studies on Cleome gynandra–comparative analysis of functional group before and after extraction" *Rom. J. Biophys*, 22(3-4), 137-143.

Liu, D, Xu, B, Zhu, J, Tang, S, Xu, F, Li, S, Jia, B, and Chen, G (2020), "Preparation of highly porous graphitic activated carbon as electrode materials for supercapacitors by hydrothermal pretreatment-assisted chemical activation" *ACS omega*, 5(19), 11058-11067.

Liu, F, Hua, S, Wang, C, Qiu, M, Jin, L, and Hu, B (2021), "Adsorption and reduction of Cr (VI) from aqueous solution using cost-effective caffeic acid functionalized corn starch" *Chemosphere*, 279130539.

Liu, H, and Yu, X (2020), "Hexavalent chromium in drinking water: Chemistry, challenges and future outlook on Sn (II)-and photocatalyst-based treatment" *Frontiers of Environmental Science & Engineering*, 14(5), 1-9.

Liu, W, and Yu, Y (2021), "Removal of recalcitrant trivalent chromium complexes from industrial wastewater under strict discharge standards" *Environmental Technology & Innovation*, 23101644.

Liu, X, Liu, H, Cui, K, Dai, Z, Wang, B, Weerasooriya, R, and Chen, X (2023a), "Adsorption-Reduction of Cr (VI) with Magnetic Fe-CN Composites" *Water*, 15(12), 2290.

Liu, X, Zhang, Y, Liu, Y, and Zhang, Ta (2023b), "Magnetic red mud/chitosan based bionanocomposites for adsorption of Cr (VI) from aqueous solutions: synthesis, characterization and adsorption kinetics" *Polymer Bulletin*, 80(2), 2099-2118.

Lohrentz, L, Bhaumik, M, and Brink, HG (2023), "High-capacity adsorption of hexavalent chromium by a polyaniline-Ni(0) nanocomposite adsorbent: Expanding the Langmuir-Hinshelwood kinetic model" *Journal of Molecular Liquids*, 389122931.

Long, Y, Chen, Z, Duvail, JL, Zhang, Z, and Wan, M (2005), "Electrical and magnetic properties of polyaniline/Fe3O4 nanostructures" *Physica B: Condensed Matter*, 370(1-4), 121-130.

Lu, J, Fan, R, Wu, H, Zhang, W, Li, J, Zhang, X, Sun, H, and Liu, D (2022), "Simultaneous removal of Cr (VI) and Cu (II) from acid wastewater by electrocoagulation using sacrificial metal anodes" *Journal of Molecular Liquids*, 359119276.

Lu, X, Zhang, W, Wang, C, Wen, T-C, and Wei, Y (2011), "One-dimensional conducting polymer nanocomposites: Synthesis, properties and applications" *Progress in Polymer Science*, 36(5), 671-712.

Ma, J, Shen, Y, Shen, C, Wen, Y, and Liu, W (2014), "Al-doping chitosan–Fe (III) hydrogel for the removal of fluoride from aqueous solutions" *Chemical Engineering Journal*, 24898-106.

MacDiarmid, AG, and Epstein, AJ (1995), "Secondary doping in polyaniline" *Synthetic Metals*, 69(1-3), 85-92.

Macherla, N, Singh, K, Nerella, M, Kumari, K, and Reddy Lekkala, RG (2022), "Improved performance of flexible supercapacitor using naphthalene sulfonic acid-doped polyaniline/sulfur-doped reduced graphene oxide nanocomposites" *International Journal of Energy Research*, 46(5), 6529-6542.

Malik, V, Saya, L, Gautam, D, Sachdeva, S, Dheer, N, Arya, DK, Gambhir, G, and Hooda, S (2022), "Review on adsorptive removal of metal ions and dyes from wastewater using tamarind-based bio-composites" *Polymer Bulletin*, 1-36.

Manjuladevi, M, Anitha, R, and Manonmani, S (2018), "Kinetic study on adsorption of Cr (VI), Ni (II), Cd (II) and Pb (II) ions from aqueous solutions using activated carbon prepared from Cucumis melo peel" *Applied water science*, 81-8.

Masindi, V, and Muedi, KL (2018), "Environmental contamination by heavy metals" *Heavy metals*, 10115-132.

McConnell, CA, Kaye, JP, and Kemanian, AR (2020), "Reviews and syntheses: Ironing out wrinkles in the soil phosphorus cycling paradigm" *Biogeosciences*, 17(21), 5309-5333.

Mema, V (2010), "Impact of poorly maintained wastewater sewage treatment plants-lessons from South Africa: Wastewater management" *ReSource*, 12(3), 60-65.

Minas, F, Chandravanshi, BS, and Leta, S (2017), "Chemical precipitation method for chromium removal and its recovery from tannery wastewater in Ethiopia" *Chem. Int*, 3(4), 291-305.

Muedi, K, Brink, H, Masindi, V, and Maree, J (2021), "Effective removal of arsenate from wastewater using aluminium enriched ferric oxide-hydroxide recovered from authentic acid mine drainage" *Journal of Hazardous Materials*, 414125491.

Muedi, KL, Masindi, V, Maree, JP, and Brink, HG (2022), "Rapid Removal of Cr (VI) from Aqueous Solution Using Polycationic/Di-Metallic Adsorbent Synthesized Using Fe3+/Al3+ Recovered from Real Acid Mine Drainage" *Minerals*, 12(10), 1318.

Muhammad, A, Shah, AuHA, and Bilal, S (2020), "Effective adsorption of hexavalent chromium and divalent nickel ions from water through polyaniline, iron oxide, and their composites" *Applied Sciences*, 10(8), 2882.

Mulvany, JG (1969), Chapter VII Membrane Filter Techniques in Microbiology. *In:* Norris, JR, and Ribbons, DW (eds.) *Methods in Microbiology.* Academic Press.

Nasar, A, and Mashkoor, F (2019), "Application of polyaniline-based adsorbents for dye removal from water and wastewater—a review" *Environmental Science and Pollution Research*, 265333-5356.

Noli, F, Dafnomili, A, Dendrinou-Samara, C, Kapnisti, M, and Pavlidou, E (2023), "Critical parameters and mechanisms of chromium removal from water by copper-based nanoparticles" *Water, Air, & Soil Pollution*, 234(1), 12.

Nowruzi, R, Heydari, M, and Javanbakht, V (2020), "Synthesis of a chitosan/polyvinyl alcohol/activate carbon biocomposite for removal of hexavalent chromium from aqueous solution" *International Journal of Biological Macromolecules*, 147209-216.

Olafadehan, OA, Bello, VE, Amoo, KO, and Bello, AM (2022), "Isotherms, kinetic and thermodynamic studies of methylene blue adsorption on chitosan flakes derived from African giant snail shell" *Afr J Environ Sci Technol*, 16(1), 37-70.

Oliveira, H (2012), "Chromium as an environmental pollutant: insights on induced plant toxicity" *Journal of Botany*.

Onu, MA, Ayeleru, OO, Oboirien, B, and Olubambi, PA (2023), "Challenges of wastewater generation and management in sub-Saharan Africa: A Review" *Environmental Challenges*, 100686.

Oruko, R, Selvarajan, R, Ogola, H, Edokpayi, J, and Odiyo, J (2020), "Contemporary and future direction of chromium tanning and management in sub Saharan Africa tanneries" *Process Safety and Environmental Protection*, 133369-386.

Owa, F (2013), "Water pollution: sources, effects, control and management" *Mediterranean journal of social sciences*, 4(8), 65.

Panneerselvam, B, and Priya K, S (2023), "Phytoremediation potential of water hyacinth in heavy metal removal in chromium and lead contaminated water" *International Journal of Environmental Analytical Chemistry*, 103(13), 3081-3096.

Peng, H, and Guo, J (2020), "Removal of chromium from wastewater by membrane filtration, chemical precipitation, ion exchange, adsorption electrocoagulation, electrochemical reduction, electrodialysis, electrodeionization, photocatalysis and nanotechnology: a review" *Environmental Chemistry Letters*, 18(6), 2055-2068.

Peng, H, Guo, J, Li, B, Liu, Z, and Tao, C (2018), "High-efficient recovery of chromium (VI) with lead sulfate" *Journal of the Taiwan Institute of Chemical Engineers*, 85149-154.

Pi, S-Y, Wang, Y, Pu, C, Mao, X, Liu, G-L, Wu, H-M, and Liu, H (2021), "Cr (VI) reduction coupled with Cr (III) adsorption/precipitation for Cr (VI) removal at near neutral pHs by polyaniline nanowires-coated polypropylene filters" *Journal of the Taiwan Institute of Chemical Engineers*, 123166-174.

Pirsaheb, M, Naderi, S, Lorestani, B, Khosrawi, T, and Sharafi, K (2014), "Efficiency of reverse osmosis system in the removal of lead, Cadmium, Chromium and Zinc in feed water of dialysis instruments in Kermanshah hospitals" *Journal of Mazandaran University of Medical Sciences*, 24(118), 151-157.

Pratush, A, Kumar, A, and Hu, Z (2018), "Adverse effect of heavy metals (As, Pb, Hg, and Cr) on health and their bioremediation strategies: a review" *International Microbiology*, 2197-106.

Pushkar, B, Sevak, P, Parab, S, and Nilkanth, N (2021), "Chromium pollution and its bioremediation mechanisms in bacteria: A review" *Journal of Environmental Management*, 287112279.

Radjenovic, J, and Sedlak, DL (2015), "Challenges and opportunities for electrochemical processes as next-generation technologies for the treatment of contaminated water" *Environmental Science & Technology*, 49(19), 11292-11302.

Rafiq, A, Ikram, M, Ali, S, Niaz, F, Khan, M, Khan, Q, and Maqbool, M (2021), "Photocatalytic degradation of dyes using semiconductor photocatalysts to clean industrial water pollution" *Journal of Industrial and Engineering Chemistry*, 97111-128.

Raghav, S, and Kumar, D (2018), "Adsorption equilibrium, kinetics, and thermodynamic studies of fluoride adsorbed by tetrametallic oxide adsorbent" *Journal of Chemical & Engineering Data*, 63(5), 1682-1697.

Rahman, Z, and Singh, VP (2019), "The relative impact of toxic heavy metals (THMs)(arsenic (As), cadmium (Cd), chromium (Cr)(VI), mercury (Hg), and lead (Pb)) on the total environment: an overview" *Environmental monitoring and assessment*, 1911-21.

Rakhunde, R, Deshpande, L, and Juneja, H (2012), "Chemical speciation of chromium in water: a review" *Critical reviews in environmental science and technology*, 42(7), 776-810.

Ranade, VV, and Bhandari, VM (2014), Industrial wastewater treatment, recycling and reuse, Butterworth-Heinemann,

Rao, DG, Senthilkumar, R, Byrne, JA, and Feroz, S (2012), Wastewater treatment: advanced processes and technologies, CRC Press,

Rashed, MN (2013), "Adsorption technique for the removal of organic pollutants from water and wastewater" *Organic pollutants-monitoring, risk and treatment*, 7167-194.

Razzak, SA, Faruque, MO, Alsheikh, Z, Alsheikhmohamad, L, Alkuroud, D, Alfayez, A, Hossain, SZ, and Hossain, MM (2022), "A comprehensive review on conventional and biological-driven heavy metals removal from industrial wastewater" *Environmental Advances*, 7100168.

Rezvani, M, Asgharinezhad, AA, Ebrahimzadeh, H, and Shekari, N (2014), "A polyaniline-magnetite nanocomposite as an anion exchange sorbent for solid-phase extraction of chromium (VI) ions" *Microchimica Acta*, 1811887-1895.

Roy, Z, and Halder, GN (2017), "Performance of Physico-chemically Activated Carbon in a Single Chamber Pressure Swing Refrigeration System" *Energy Procedia*, 109393-400.

Samuel, MS, Shah, SS, Subramaniyan, V, Qureshi, T, Bhattacharya, J, and Singh, NP (2018), "Preparation of graphene oxide/chitosan/ferrite nanocomposite for Chromium (VI) removal from aqueous solution" *International Journal of Biological Macromolecules*, 119540-547.

Sarayu, K, and Sandhya, S (2012), "Current technologies for biological treatment of textile wastewater–a review" *Applied biochemistry and biotechnology*, 167645-661.

Scheele, CW (1777), Chemische Abhandlung von der Luft und dem Feuer, Verlegt von Magn. Swederus, Buchhändler zu finden bey SL Crusius,

Schweitzer, L, and Noblet, J (2018), Water contamination and pollution. *Green chemistry.* Elsevier.

Semghouni, H, Bey, S, Figoli, A, Criscuoli, A, Benamor, M, and Drioli, E (2020), "Chromium (VI) removal by Aliquat-336 in a novel multiframe flat sheet membrane contactor" *Chemical Engineering and Processing-Process Intensification*, 147107765.

Shanmugavel, T, Raj, SG, Rajarajan, G, and Kumar, GR (2014), "Tailoring the structural and magnetic properties and of nickel ferrite by auto combustion method" *Procedia materials science*, 61725-1730.

Sharma, N, Sodhi, KK, Kumar, M, and Singh, DK (2021), "Heavy metal pollution: Insights into chromium eco-toxicity and recent advancement in its remediation" *Environmental Nanotechnology, Monitoring & Management*, 15100388.

Shekhar Sarker, S, Akter, T, Parveen, S, Tushar Uddin, M, Kanti Mondal, A, and Sujan, SMA (2023), "Microalgae-based green approach for effective chromium removal from tannery effluent: A review" *Arabian Journal of Chemistry*, 16(10), 105085.

Shekhawat, K, Chatterjee, S, and Joshi, B (2015), "Chromium toxicity and its health hazards" *Int. J. Adv. Res*, 3(7), 167-172.

Shrestha, R, Ban, S, Devkota, S, Sharma, S, Joshi, R, Tiwari, AP, Kim, HY, and Joshi, MK (2021), "Technological trends in heavy metals removal from industrial wastewater: A review" *Journal of environmental chemical engineering*, 9(4), 105688.

Singh, A, Guleria, A, Neogy, S, and Rath, MC (2020), "UV induced synthesis of starch capped CdSe quantum dots: Functionalization with thiourea and application in sensing heavy metals ions in aqueous solution" *Arabian Journal of Chemistry*, 13(1), 3149-3158.

Singh, N, Agrawal, S, and Rachna, K (2019), "Methylene blue dye removal from water by nickel ferrite polyaniline nanocomposite".

Singh, P, Mohan, B, Madaan, V, Ranga, R, Kumari, P, Kumar, S, Bhankar, V, Kumar, P, and Kumar, K (2022), "Nanomaterials photocatalytic activities for waste water treatment: a review" *Environmental Science and Pollution Research*, 29(46), 69294-69326.

Singh, P, and Shukla, S (2020), "Advances in polyaniline-based nanocomposites" *Journal of Materials Science*, 55(4), 1331-1365.

Strathmann, H (2010), "Electrodialysis, a mature technology with a multitude of new applications" *Desalination*, 264(3), 268-288.

Terraza, C, Martín Trasancos, R, Saldias, C, Gonzalez, M, and Leiva, A (2018), "Preparation of CuONPs@PVDF/Non-Woven Polyester Composite Membrane: Structural Influence of Nanoparticle Addition" *Polymers*, 10862.

Tran, HNaYSJaCHP (2016), "Thermodynamic parameters of cadmium adsorption onto orange peel calculated from various methods: A comparison study" *Journal of Environmental Chemical Engineering*, 4(3), 2671--2682.

Tripathy, S, Sahu, S, Patel, RK, Panda, RB, and Kar, PK (2021), "Efficient removal of Cr (VI) by polyaniline modified biochar from date (Phoenix dactylifera) seed" *Groundwater for Sustainable Development*, 15100653.

Tumolo, M, Ancona, V, De Paola, D, Losacco, D, Campanale, C, Massarelli, C, and Uricchio, VF (2020), "Chromium pollution in European water, sources, health risk, and remediation strategies: an overview" *International journal of environmental research and public health*, 17(15), 5438.

Verma, M, Lee, I, Hong, Y, Kumar, V, and Kim, H (2022), "Multifunctional β-Cyclodextrin-EDTA-Chitosan polymer adsorbent synthesis for simultaneous removal of heavy metals and organic dyes from wastewater" *Environmental Pollution*, 292118447.

Wang, M, Liu, X, Pan, B, and Zhang, S (2013), "Photodegradation of Acid Orange 7 in a UV/acetylacetone process" *Chemosphere*, 93(11), 2877-2882.

Webb, PA (2003), "Introduction to chemical adsorption analytical techniques and their applications to catalysis" *Micromeritics Instrument Corp. Technical Publications*, 1-12.

Worch, E (2021), Adsorption Technology in Water Treatment : Fundamentals, Processes, and Modeling. 2nd, Revised Edition. ed. Berlin ;: De Gruyter.

Xia, S, Song, Z, Jeyakumar, P, Shaheen, SM, Rinklebe, J, Ok, YS, Bolan, N, and Wang, H (2019), "A critical review on bioremediation technologies for Cr (VI)-contaminated soils and wastewater" *Critical reviews in environmental science and technology*, 49(12), 1027-1078.

Xu, C, Xu, Y, Zhong, D, Chang, H, Mou, J, Wang, H, and Shen, H (2022a), "Efficient adsorption and reduction of Cr (VI) by Zr4+ cross-linked magnetic chitosan/polyaniline composite" *Journal of environmental chemical engineering*, 10(6), 108977.

Xu, K, Li, L, Huang, Z, Tian, Z, and Li, H (2022b), "Efficient adsorption of heavy metals from wastewater on nanocomposite beads prepared by chitosan and paper sludge" *Science of the Total Environment*, 846157399.

Yang, G, Tang, L, Cai, Y, Zeng, G, Guo, P, Chen, G, Zhou, Y, Tang, J, Chen, J, and Xiong, W (2014), "Effective removal of Cr (VI) through adsorption and reduction by magnetic mesoporous carbon incorporated with polyaniline" *RSC advances*, 4(102), 58362-58371.

Yuan, H, Zhou, H, Zhao, Y, Tan, H, Antoine, R, and Zhang, S (2022), "Metal-Organic frameworks encapsulated Ag Nanoparticle-Nanoclusters with enhanced luminescence for simultaneous detection and removal of Chromium (VI)" *Microchemical Journal*, 181107722.

Yuan, Y, Zhu, W, Du, G, Wang, D, Zhu, J, Zhu, X, and Pezzotti, G (2018), "Two-step method for synthesizing polyaniline with bimodal nanostructures for high performance supercapacitors" *Electrochimica Acta*, 282286-294.

Zare, N, Kojoori, RK, Abdolmohammadi, S, and Sadegh-Samiei, S (2022), "Ultrasonic-assisted synthesis of highly effective visible light Fe3O4/ZnO/PANI nanocomposite: Thoroughly kinetics and thermodynamic investigations on the Congo red dye decomposition" *Journal of Molecular Structure*, 1250131903.

Zaynab, M, Al-Yahyai, R, Ameen, A, Sharif, Y, Ali, L, Fatima, M, Khan, KA, and Li, S (2022), "Health and environmental effects of heavy metals" *Journal of King Saud University - Science*, 34(1), 101653.

Zhang, Y-H, Liu, C-S, Tian, Y, Wang, J, Xin, S, and Sheng, X (2023), "An eco-friendly photo-responsive hyaluronic acid-based supramolecular polysaccharide hybrid hydrogels for plant growth regulation and heavy metal ions adsorption" *International Journal of Biological Macromolecules*, 242125194.

Zhao, C, Liu, G, Tan, Q, Gao, M, Chen, G, Huang, X, Xu, X, Li, L, Wang, J, Zhang, Y, and Xu, D (2023), "Polysaccharide-based biopolymer hydrogels for heavy metal detection and adsorption" *Journal of Advanced Research*, 4453-70.

Zhitkovich, A (2011), "Chromium in drinking water: sources, metabolism, and cancer risks" *Chemical research in toxicology*, 24(10), 1617-1629.

Zhu, K, Gao, Y, Tan, X, and Chen, C (2016), "Polyaniline-modified Mg/Al layered double hydroxide composites and their application in efficient removal of Cr (VI)" *ACS Sustainable Chemistry & Engineering*, 4(8), 4361-4369.